GEORGIA INSTITUTE OF TECHNOLOGY
School of Civil Engineering
Atlanta, Georgia

FINAL REPORT

PROJECT B-608

HYDRODYNAMICS OF TIRE HYDROPLANING

By

C. S. MARTIN

GRANT NGR-11-002-033

1 JULY 1965 to 30 JUNE 1966
Issued 15 June 1966

Performed for
NATIONAL AERONAUTICS AND SPACE ADMINISTRATION
WASHINGTON, D. C.

FOREWORD

This report was prepared by the School of Civil Engineering of the Georgia Institute of Technology under NASA Grant NGR-11-002-033. The personnel of the Langley Research Center of the National Aeronautics and Space Administration gave technical advice and assistance in the course of this grant. Of especial assistance were Messrs. W. B. Horne and U. T. Joyner.

The analytical work for this grant was performed under the supervision of Dr. C. S. Martin, Assistant Professor in the School of Civil Engineeering. The experimental data presented for comparison was collected by the personnel of the Langley Research Center. The author would like to acknowledge the assistance of Messrs. M. M. Aikenhead, A. S. Ardila, A. E. Cardoso and D. L. Whitt in the preparation of this report.

ABSTRACT

2 4730

The hydrodynamics of pneumatic tire hydroplaning are explained from a purely analytical standpoint. Lift and drag forces on an assumed planing surface (tire) are obtained for an ideal fluid undergoing two-dimensional motion. For the condition of incipient hydroplaning the theoretical lift coefficient is found to be 0.8, compared to a value of 0.7 from experiment. The lift and drag coefficients are shown to decrease as the tire lifts further off the runway. The pressure distribution on the pavement from theory compares favorably with the experimental results.

Author

TABLE OF CONTENTS

LIST OF FIGURES

INTRODUCTION

The planing or skiing of a pneumatic airplane tire has, on numerous occasions, placed pilots in rather precarious situations. This phenomenon of tire hydroplaning can also be of concern to motorists cruising at relatively high speeds (50-60 mph) on flooded highway pavements. Tire hydroplaning results from the large water pressures developed between the tire and pavement surface. Whenever the total hydrodynamic force developed from the distributed water pressure on the tire equals the total load the tire is carrying, hydroplaning occurs. The tire then loses contact with the pavement and essentially skis on the water. The comprehensive experimental work on tire hydroplaning by the personnel of the Langley Research Center of the National Aeronautics and Space Administration is of a pioneering nature. Horne and Dreher (1) summarize recent experiment research on tire hydroplaning. The purpose of this investigation is to explain tire hydroplaning from a standpoint of theoretical hydrodynamics. Prior to developing the theory, the pertinent fluid variables are discussed. Finally the theoretical results are compared with existing experimental results.

DISCUSSION OF HYDRODYNAMIC VARIABLES

All of the manifestations of tire hydroplaning are comprehensively discussed by Horne and Dreher. It is quite obvious though that not only the hydrodynamics of the flow, but also the elasticity of the tire should be included in a general theory. In this investigation, only the hydrodynamic part of the problem is considered. The shape of the tire will be considered to be fixed for this initial study.

The hydrodynamic or lift force exerted on the tire by the water is a function of the following geometric, flow, and fluid variables

$$F_L = f\ (A,\ D,\ U,\ \rho,\ \gamma,\ \sigma,\ \mu) \tag{1}$$

in which A is a characteristic area on which the water pressure acts and is a function of tire geometry, D is the depth of water on the pavement, U is the translational speed of the tire, and ρ, γ, σ, and μ are the mass density, specific weight, surface tension, and dynamic viscosity of the water, respectively. The lift force can be represented by

$$F_L = C_L\ A\ \frac{\rho U^2}{2} \tag{2}$$

in which C_L can be shown from dimensional analysis to be a function of the following variables

$$C_L = f'\ (N_F,\ N_W,\ N_R,\ \text{Tire Geometry}) \tag{3}$$

The quantities N_F, N_W, and N_R are the dimensionless parameters Froude number, Weber number, and Reynolds number, respectively. Each of these parameters

represents the relative significance of the mass density to each of the other three fluid properties. The relative significance of each of the four fluid properties present in tire hydroplaning is discussed in the following.

a) Mass density. The density of the water becomes an obvious significant fluid property in tire hydroplaning because of the severe curvature of the streamlines in the vicinity of the tire and the high speeds involved.

b) Specific weight. The existence of a free surface introduces the effect of gravity into the problem as well as surface tension. The effect of gravity on fluid-flow patterns can be represented by the well-known Froude number, which is proportional to the ratio of fluid-inertia force to fluid-weight force, defined as

$$N_F = \frac{U}{\sqrt{gL}} \tag{4}$$

in which g is the acceleration of gravity, and L is a characteristic length. For tire hydroplaning the suitable choice of characteristic velocity and length would be the translational speed of the tire, U, and the depth of water, D, on the pavement, respectively. Inasmuch as hydroplaning normally occurs for high speeds ($\gtrsim$ 40 mph) and at shallow-water depths the Froude number can be considered to be quite large. As discussed by Rouse (2) gravity-type flows at large Froude numbers can be well represented from analyses for which gravity as a variable is absent. The effect of gravity on tire hydroplaning is believed to be insignificant in the usual situation, and will not be included in the theory.

c) _Surface tension._ As with specific weight, the liquid-gas property of surface tension is present as a variable because of the existence of the liquid-gas interface, the free surface. The effect of surface tension can be represented by the Weber number, a dimensionless parameter which can be defined as being proportional to the ratio of fluid-inertia force to fluid surface-tension force. The Weber number is defined here as

$$N_W = \frac{U}{\sqrt{\sigma/\rho L}} \qquad (5)$$

For the hydroplaning problem U would logically be the translational speed of the tire, and L the depth of water on the pavement, D. Surface tension affects motion only for small values of the Weber number and, more particularly, for small radii of curvature of the water surface. Inasmuch as the velocity U is large and the depth D is small it is not readily apparent that the Weber number will be either large or small. For large values of the Weber number the effect of surface tension is insignificant and can be neglected in analyses. It is believed, however, that surface tension does not appreciably affect the pressure and, consequently, is not an important parameter for tire hydroplaning. It is true, of course, that surface tension is the cause of the breakup of the jet that leaves the vicinity of the tire in the form of a spray. This breakup is not believed, however, to affect the magnitude of the lift on the tire. The theory that follows is based on the assumption that surface tension is insignificant.

d) _Viscosity._ Since all fluids possess viscosity its inclusion or exclusion from a theory must be seriously considered. The well-known

Reynolds number, which is a ratio of fluid-inertia force to fluid-viscous force, represents the relative importance of the two fluid properties, mass density and viscosity. The Reynolds number

$$N_R = \frac{\rho UL}{\mu} .$$ (6)

The characteristic length would logically be the spacing between the tire and pavement when total hydroplaning occurred. The translational speed U is usually large and the viscosity of water is quite low, meaning that, except for very small values of L, the Reynolds number will be large. The effect of viscosity becomes insignificant for high Reynolds numbers and can rightly be neglected as a variable. Viscosity would be expected to play somewhat of a role for slightly damp (and if oily as just after a rain) pavements on which slipping from lubrication can take place. In this case hydroplaning or slipping is greatly augmented if the tires are smooth. On the other extreme, that is flooded pavements, the density of the water would be the expected significant fluid property. These two extremes of thin film and viscosity effect and moderate to flooded depth and density effect have been discussed by Horne and Dreher to some extent. The normal situation for aircraft seems to be one for which the water depth is more than thin-film and the tire is not smooth, but grooved. The grooves allow for escape of the water under high pressure, thereby delaying hydroplaning.

The mass density of the water is assumed to be the significant and the only fluid property present in the proposed theory. This assumption is strengthened by the experimental results of Horne and Dreher. If the characteristic area of equation (2) is represented by the static footprint

area and U by the velocity of the vehicle at the incipient condition of the hydroplaning, Horne and Dreher found that C_L is essentially a constant, 0.7. Their results are from tests covering a range of inflation tire pressures from 24 psi to 150 psi, of vehicle speeds from 45 mph to 120 mph, and of lift force F_L (which is equal and opposite to the vehicle weight force) from 925 lb. to 22,000 lb. Their results prove that, for the tests run at least, the fluid mass density is the sole fluid property affecting motion and, furthermore, strongly indicate that the flow pattern in the vicinity of the tire was essentially similar for all tests. The latter statement follows from the fact that C_L was essentially constant for all tires.

THEORY

The foregoing discussion on the significance of the various fluid-property variables present led to the conclusion that, for moderate water depths and vehicle speeds, the fluid density is the significant fluid variable. Such a condition in essence specifies the assumption of an ideal fluid. If such an assumption is justified no more liberty would be taken if, further, the flow is assumed to be irrotational. The conditions for potential flow are now satisfied. The velocity potential is defined by

$$\vec{V} = \overrightarrow{grad} \; \varphi = \vec{\nabla} \; \varphi \tag{7}$$

in which $\vec{V}$ is the velocity at any point and φ the velocity potential. In order that the useful tool of complex variables may be utilized the flow is further assumed to be two-dimensional. Considerable liberty is taken with this assumption as the actual flow under and around a tire is definitely three-dimensional. It is obvious that the results of the two-dimensional theory will have to be interpreted with caution in applying them to the actual three-dimensional problem.

For two-dimensional motion in rectangular coordinates the velocity potential is defined as

$$u = \frac{\partial \varphi}{\partial x} \; , \; v = \frac{\partial \varphi}{\partial y} \tag{8}$$

in which u and v are the horizontal and vertical components of the total velocity V, in the x- and y-directions, respectively. The stream function ψ is defined as

$$u = \frac{\partial \psi}{\partial y}, \quad v = -\frac{\partial \psi}{\partial x} \tag{9}$$

Laplace's equation is satisfied for both φ and ψ

$$\nabla^2 \varphi = \frac{\partial^2 \varphi}{\partial x^2} + \frac{\partial^2 \varphi}{\partial y^2} = 0 \,, \tag{10}$$

and

$$\nabla^2 \psi = \frac{\partial^2 \psi}{\partial x^2} + \frac{\partial^2 \psi}{\partial y^2} = 0 \tag{11}$$

The dynamical equation of Bernoulli

$$\frac{\rho}{2}(u^2 + v^2) + p = p_0 \tag{12}$$

in which p is the water pressure at any point and p_0 is the reference pressure, which in this instance is atmospheric. Once the potential field represented by φ and/or ψ is found the dynamical quantities such as pressure variation, lift, and drag can be determined from Bernoulli's equation.

The hydroplaning problem is one of unsteady flow to the stationary observer. The problem can be transformed into one of steady motion simply by changing the axis of reference to the tire. The picture now seen is that of a jet of constant depth D and infinite width striking a curved surface (tire) which is slightly above or in contact with a plane surface as shown in Figure 1.[*] This steady-flow problem is dynamically identical to the unsteady-flow hydroplaning problem of the tire translating at the same speed, U. When the tire is in contact with the pavement, partial hydroplaning is said to exist; when

---

[*] All illustrations are in Appendix A.

there is a space between the tire and the pavement total hydroplaning is said to exist. The theory here is for the more general case of total hydro-planing, of which partial hydroplaning is a special case.

The hydrodynamic problem depicted in Figure 1 is that of free-streamline flow with a curved boundary. From Bernoulli's theorem the velocity everywhere on the water surface has the constant value of U as gravity is neglected. The lift force on the tire can be determined by integrating the pressure distribution thereon. The drag force can be either determined from the pressure distribution on the tire or from a simple momentum analysis involving the unknown downstream depth, d, and the angle of the jet at infinity. These two quantities are not known a priori and depend solely on the tire shape and tire-position relative to the pavement. The elasticity of the tire and the vehicle weight are not explicity nor directly taken into account. The tire is assumed to be flexible and deformed out of its original circular shape but no dynamic balance between water pressure, air-inflation pressure, tire elasticity, tire-rotating effects, and tire shape is made. Furthermore, no attempt is made to effect a dynamic balance of lift force and vehicle weight force which dictates the clearance or space between tire and pavement at the downstream exit. The theory herein is simply a hydrodynamical one for which forces are determined for an assumed shape and assumed position of the shape relative to the pavement.

Conformal Representation - The theory of complex variables through the means of conformal representation is a useful technique for many two-dimensional free-streamline problems for which irrotational flow may be assumed. The so-called physical plane, or z-plane

$$z = x + iy \qquad (13)$$

is depicted in Figure 1 for the case of a jet striking the curved surface.
Point A is at minus infinity and point B at plus infinity. At points C and
E the fluid is assumed to separate from the tire. Point D is a stagnation
point. Theoretically point F is also at infinity. At point G the velocity
reaches its minimum value on the pavement. At points A, B, and F the velocity
is U.

The complex-potential plane defined as

$$w = \varphi + i\psi \qquad (14)$$

is shown in Figure 2. Point D is arbitrarily given a value of φ of 0. The
stream function ψ is assigned a value of 0 on AB. The values of the other
points in the plane are self-explanatory.

The dimensionless complex velocity

$$\zeta = \frac{1}{U} \frac{dw}{dz} = \frac{u}{U} - i \frac{v}{U} = \frac{V}{U} e^{i\delta} \qquad (15)$$

comprises the hodograph plane, as shown in Figure 3. The angle that the
fluid velocity makes with the x-axis is δ, which is defined as

$$\delta = \tan^{-1}(v/u) \qquad (16)$$

In the hodograph plane lines AFE and BC are arcs of a circle of unit radius
inasmuch as they are free streamlines for which V = U. The line AGB forms
a slit as G is a point of minimum velocity on the pavement. Line CDE is
curved in the hodograph plane as both the angle δ and the velocity V are
changing on the curved tire surface. Point F can be either in the third or

fourth quadrant, depending on whether $\delta_F > \pi/2$ or $\delta_F < \pi/2$, respectively.

The function

$$\Omega = \ln \zeta = \ln \frac{V}{U} - i\delta \qquad (17)$$

constitutes the logarithmic hodograph plane, shown in Figure 4. Lines AFE and BC are straight as $\ln V/U = 0$. Similarily lines AG and GB are straight as $\delta = 0$. On CD and ED, however, the logarithmic-hodograph lines are curved as both δ and $\ln V/U$ are varying. This fact extremely complicates the problem of conformal representation as the exact shape of lines CD and DE in the log-hodograph plane are not known a priori. Furthermore the usual practice of using the Schwartz-Christoffel transformation is precluded because of these non-polygonal lines in the log-hodograph plane.

Since the classical approach to free-streamline hydrodynamics is precluded two alternatives were considered. The first involved the strictly head-on approach of direct numerical analysis, involving finite-difference equations and/or relaxation techniques. The second alternative was to use an untried approach. The latter alternative was chosen with the idea that in addition to solving the immediate problem a possible contribution could be made to the area of free-streamline theory with curved boundaries.

Solution in Terms of δ and $\ln V/U$ - The technique to be used is based on the fact that all analytic functions satisfy Laplace's equation in the respective planes. Since

$$\Omega = \ln \zeta = \ln \left[\frac{1}{U} \frac{dw}{dz} \right]$$

10

is an analytic function if only the single-valued part of the ln-function is used, it follows that

$$\nabla^2 \delta = \frac{\partial^2 \delta}{\partial x^2} + \frac{\partial^2 \delta}{\partial y^2} = 0 \qquad (18)$$

and

$$\nabla^2 \left[\ln \frac{V}{U}\right] = \frac{\partial^2 \left[\ln \frac{V}{U}\right]}{\partial x^2} + \frac{\partial^2 \left[\ln \frac{V}{U}\right]}{\partial y^2} = 0 \qquad (19)$$

These two equations constitute a boundary-value problem for δ and/or $\ln V/U$ in the z-plane. Inasmuch as the location of the free-streamlines are not known a priori this change in dependent variables does not simplify the problem. In the w, or complex-potential, plane, however, the boundaries on φ and ψ are known a priori. It is also apparent that, from the theory of analytic functions

$$\nabla^2 \delta = \frac{\partial^2 \delta}{\partial \varphi^2} + \frac{\partial^2 \delta}{\partial \psi^2} = 0 \qquad (20)$$

and

$$\nabla^2 \left[\ln \frac{V}{U}\right] = \frac{\partial^2 \left[\ln \frac{V}{U}\right]}{\partial \varphi^2} + \frac{\partial^2 \left[\ln \frac{V}{U}\right]}{\partial \psi^2} = 0 \qquad (21)$$

In Figures 5 and 6 the boundary conditions for δ and $\ln V/U$ are shown. On line AGB the angle of the streamline $\delta = 0$ whereas $\ln V/U$ varies, reaching a minimum at G. Incidentally, point G does not necessarily have to be represented as a point in the subsequent analysis as the hodograph planes are

11

not used. On the free-streamlines AFE and BC ln V/U = 0 and δ varies. On
line CDE both δ and ln V/U are varying. It should be noted that at D ln V/U
approaches minus infinity and δ has a step discontinuity of π as the fluid
leaving D for C has the opposite direction than that leaving for E. Either
δ or ln V/U can be arbitrarily specified on CDE. The boundary-value pro-
blem for δ and/or ln V/U in the w-plane is much simpler than in the z-plane
because of the straight lines forming the boundaries on the w-plane. The
boundary-value problem can be formulated for δ on all lines by use of the
Cauchy-Riemann equations on lines AFE and BC. The equations in this instance
are

$$\frac{\partial \delta}{\partial \psi} = \frac{\partial \left[\ln \frac{V}{U} \right]}{\partial \varphi} \tag{22a}$$

and

$$\frac{\partial \delta}{\partial \varphi} = - \frac{\partial \left[\ln \frac{V}{U} \right]}{\partial \psi} \tag{22b}$$

On lines AFE and BC ln V/U = 0. By the first Cauchy-Riemann equation $\partial \delta / \partial \psi$ =
0 on AFE and BC. The boundary-value problem for δ in the w-plane is shown in
Figure 6. On CDE δ is specified by an arbitrary function. Since the boundary
conditions on lines DCB and DEF are not homogeneous, that is both Dirichlet-
and Neumann-type boundary conditions are specified on the same line, classic
techniques for solving $\nabla^2 \delta = 0$ in the w-plane are not very useful.

The problem of mixed boundary conditions on DCB and DEF can be alleviated
by transforming the w-plane into another plane for which all straight lines
have only single boundary conditions. The transformed plane will be called

the w'-plane, where $w' = \varphi' + i\psi'$. Its dimensionless counterpart is the w_1-plane, where $w_1 = w'/\varphi'_B = \varphi_1 + i\psi_1$. In order that the w_1-plane satisfy the above condition it must have the shape of a rectangle, as shown in Figure 7. On line AB the Dirichlet condition is $\delta = 0$. On lines AFE and BC the Neumann condition of $\partial\delta/\partial\varphi_1 = 0$ must be satisfied. The boundary conditions on these three lines can be obtained from a theorem of conformal mapping, which states that under transformation of an analytic function (Ω) boundary conditions on a function (δ) of the type $\delta = $ constant and $\overrightarrow{\text{grad}}\ \delta = 0$ remain invariant, Churchill (3). On CDE or EDC, however, δ varies. The function for δ on EDC will not remain invariant under transformation from the w-plane to the w_1-plane. Since δ is to be arbitrary on EDC it will be specified in terms of φ_1 in the w_1-plane.

The boundary-value problem now becomes one of a solution to

$$\nabla^2\delta = \frac{\partial^2\delta}{\partial\varphi_1^2} + \frac{\partial^2\delta}{\partial\psi_1^2} = 0 \tag{23}$$

in a rectangle. The technique of Fourier series will be utilized to effect the solution for arbitrary functions of δ on EDC. Since

$$\Omega = \ln\left[\frac{1}{U}\frac{dw}{dz}\right],$$

and

$$w = w(w_1),$$

$$\Omega = \ln\left[\frac{1}{U}\frac{dw_1}{dz}\frac{dw}{dw_1}\right],$$

13

or

$$dz = \frac{1}{U} e^{-\Omega} \frac{dw}{dw_1} dw_1 \tag{24}$$

The solution for $\delta = \delta(\varphi_1, \psi_1)$ in the w_1-plane and the determination of its harmonic conjugate $\ln V/U$ enables the determination of Ω as a function of w_1. From the transformation $w = w(w_1)$ the derivative dw/dw_1 can be obtained. Upon integrating equation (24) the shape of the curved surface (tire) in the z-plane can be obtained.

In order that the w-plane can be transformed into the w_1-plane an intermediate plane is necessary. This plane is depicted in Figure 8 and it called the t-plane. The Schwartz-Christoffel transformation can be used to connect the t-plane to both the w-plane and the w_1-plane as the latter two planes are closed polygons. Since there are a total of six points in each plane (it is not necessary to include point G as it is not a corner in either the w- or w_1-plane), and three points may be located arbitrarily in the t-plane, three points have to have variable values on the real axis of the t-plane. The arbitrary points are chosen to be A, B, and E, located at 0, 1 and infinity, respectively. Point F is located at - a, where a can take on any value between 0 and ∞. Point C is located at t_c. At point D, t = b, which can vary from approximately t_c to ∞. Using the Schwartz-Christoffel transformation to connect the t-plane with the w-plane

$$\frac{dw}{dt} = \frac{A(t - b)}{t(t - 1)(t + a)} \tag{25}$$

in which A is a complex constant. By using partial fractions

$$\frac{dw}{dt} = A \left\{ \frac{t - b}{a(1 + a)(t + a)} + \frac{t - b}{(1 + a)(t - 1)} - \frac{t - b}{at} \right\}$$

Upon integrating and simplifying

$$w = A \left\{ \frac{b}{a} \ln t - \frac{b - 1}{1 + a} \ln(t - 1) - \frac{(a + b)}{a(1 + a)} \ln(t + a) \right\} + B \qquad (26)$$

in which B is a complex constant of integration. The constant A can be evaluated at point A to be

$$A = \frac{a}{b} \frac{UD}{\pi}$$

At point B it is found that

$$\frac{d}{D} = \frac{a}{b} \frac{b - 1}{1 + a} \qquad (27)$$

At point E the constant of integration can be evaluated to be

$$B = \varphi_E + iUd$$

The complex-potential function becomes

$$w = \frac{UD}{\pi} \left\{ \ln t - \frac{a}{b} \frac{b - 1}{1 + a} \ln(t - 1) - \frac{(a + b)}{b(1 + a)} \ln(t + a) \right\} + \varphi_E + iUd$$

or

$$w = \frac{UD}{\pi} \ln t - \frac{Ud}{\pi} \ln(t - 1) - \frac{U(D - d)}{\pi} \ln(t + a) + \varphi_E + iUd \qquad (28)$$

The latter expression is clearly the analytic function for a source of strength UD/π at A, a sink of strength Ud/π at B, and a sink of strength $U(D - d)/\pi$ at F, all in the t-plane.

By transforming the t-plane to the w_1-plane

$$\frac{dw_1}{dt} = \frac{A'}{\sqrt{t}\ \sqrt{t-1}\ \sqrt{t-t_c}} \qquad (29)$$

in which A' is a complex constant. From the theory of elliptic functions, Bowman (4), it is apparent that if $t_c = 1/k^2$, in which k is the modulus of Jacobian elliptic functions, the above expression can be integrated in terms of elliptic functions. From Byrd and Friedman (5) or Bowman

$$w_1 = \frac{1}{K}\ sn^{-1}\ \left[\sqrt{t}\right] \qquad (30)$$

in which K is the complete elliptic integral of the first kind and sn is the sine-amplitude Jacobian elliptic function. The inverse relationship

$$t = sn^2\ [Kw_1,\ k] = sn^2\ [Kw_1] \qquad (31)$$

In the w_1-plane φ_{1B} has been made unity. It follows from the transformation of a rectangle into the upper half of the t-plane that $\psi_{1EDC} = K'/K$ in which K' is the complementary elliptic integral of the first kind. Since $K = K(k)$ and $K' = K(k')$, in which k' is the complementary modulus related to the modulus by

$$k'^2 = 1 - k^2, \qquad (32)$$

it follows that by changing k the aspect ratio of the rectangle in the w_1-plane changes. The value of a and b in the t-plane can be determined from the

16

location of points F and D in the w_1-plane. Hence

$$a = - sn^2(iK\psi_{1F})$$ (33)

and

$$b = sn^2(K\varphi_{1D} + iK') = \frac{1}{k^2 sn^2(K\varphi_{1D})}$$ (34)

From the differentiation relationships for Jacobian elliptic functions

$$\frac{dw_1}{dt} = \frac{1}{2K[sn(Kw_1) cn(Kw_1) dn(Kw_1)]}$$ (35)

in which cn is the cosine-amplitude and dn the delta-amplitude function. The three functions are related by

$$sn^2(Kw_1) + cn^2(Kw_1) = 1$$ (36a)

and

$$k^2 sn^2(Kw_1) + dn^2(Kw_1) = 1$$ (36b)

The relationship for dw/dw_1 can be expressed entirely in terms of Jacobian elliptic functions with Kw_1 as the argument

$$\frac{dw}{dw_1} = 2K \frac{a}{b} \frac{UD}{\pi} \left[\frac{b - sn^2(Kw_1)}{a + sn^2(Kw_1)} \right] \left[\frac{dn(Kw_1)}{sn(Kw_1) cn(Kw_1)} \right]$$ (37)

The solution for $\Omega(w_1)$ is determined by inspection once δ is found from

17

the boundary-value problem formulated in the w_1-plane. Applying separation of variables technique to equation (23) a possible solution is

$$\delta = (c_1 \sinh \beta\psi_1 + c_2 \cosh \beta\psi_1)(c_3 \sin \beta\varphi_1 + c_4 \cos \beta\varphi_1) \qquad (38)$$

in which β is a constant to be determined from the boundary conditions. For $\beta = 0$ the separate solution

$$\delta = (b_1 \psi_1 + b_2)(b_3\varphi_1 + b_4) \qquad (39)$$

The boundary conditions are

$$AB : \quad \psi_1 = 0 \quad ; \quad \delta = 0$$

$$AFE: \quad \varphi_1 = 0 \quad ; \quad \partial\delta/\partial\varphi_1 = 0$$

$$BC : \quad \varphi_1 = 1 \quad ; \quad \partial\delta/\partial\varphi_1 = 0$$

$$EDC: \quad \psi_1 = K'/K; \quad \delta = f(\varphi_1)$$

in which $f(\varphi_1)$ is an arbitrary function, discontinuous at D; it can be related to a continuous function $g(\varphi_1)$ by

$$[f(\varphi_1)]_{ED} = \pi - g(\varphi_1) \qquad (40a)$$

$$[f(\varphi_1)]_{DC} = \quad - g(\varphi_1) \qquad (40b)$$

For $\beta = 0$ the boundary condition on AB requires that $b_2 = 0$. The Neumann boundary condition on AFE and BC requires that $b_3 = 0$. On EDC

$$\delta = f(\varphi_1) = b_1 b_4 \psi_{1EDC} = A_o \qquad (41)$$

18

From the theory of Fourier series, Churchill (6)

$$A_o = \int_0^1 f(\varphi_1)d\varphi_1 = \pi\varphi_{1D} - \int_0^1 g(\varphi_1)d\varphi_1 \tag{42}$$

For $\beta \neq 0$, the boundary condition on AB requires that $c_2 = 0$. For the boundary condition on AFE to be satisfied $c_3 = 0$. On BC the Neumann boundary condition means that $\sin \lambda = 0$. Hence $\lambda = n\pi$; $n = 1,2,3,\ldots$. The total solution in terms of Fourier series

$$\delta = A_o \frac{K}{K'} \psi_1 + \sum_{n=1}^{\infty} A_n \sinh n\pi\psi_1 \cos n\pi\varphi_1 \tag{43}$$

The coefficient A_n is determined from the boundary condition on EDC

$$A_n \sinh(n\pi K'/K) = 2 \int_0^1 f(\varphi_1) \cos n\pi\varphi_1 d\varphi_1$$

$$\tag{44}$$

$$= \frac{2}{n} \sin n\pi\varphi_{1D} - 2 \int_0^1 g(\varphi_1) \cos n\pi\varphi_1 d\varphi_1$$

It will be shown later that A_o must be 0 in order that $\ln V/U = 0$ on both AFE and BC. The boundary condition on BC will fix the location of D in the w_1-plane.

The function $f(\varphi_1)$ must be specified such that the boundary EDC has the proper curvature and resembles the deformed portion of a tire. Three separate elementary functions were tried in an attempt to produce a curved boundary on EDC that resembles a hydroplaning tire. The final relationship for dz is

19

expressed in terms of the solution for a flat plate times an expression including the effect of curvature. Since the effect of curvature can be included in one term the flat-plate solution will be effected first. For a flat plate inclined at an angle θ with the approaching flow

$$[f(\varphi_1)]_{ED} = \pi - \theta \tag{45a}$$

$$\text{and} \quad [f(\varphi_1)]_{DC} = -\theta \tag{45b}$$

In this case the continuous function $g(\varphi_1)$ is a constant, θ.

The coefficient

$$A_o = \pi \int_0^{\varphi_{1D}} d\varphi_1 - \theta \int_0^1 d\varphi_1 \tag{46}$$

$$= \pi \varphi_{1D} - \theta$$

The coefficient A_n is determined from

$$A_n \sinh(n\pi K'/K) = 2\pi \int_0^{\varphi_{1D}} \cos n\pi\varphi_1 d\varphi_1 - 2\theta \int_0^1 \cos n\pi\varphi_1 d\varphi_1$$

$$= \frac{2}{n} \sin n\pi\varphi_{1D}$$

From the theory of Jacobian elliptic functions Jacobi's nome is defined as

$$q = \exp(-\pi K'/K) \; ; \; 0 < q < 1 \tag{47}$$

Hence,

$$\sinh(n\pi K'/K) = \frac{1}{2} [q^{-n} - q^n]$$

and

$$A_n = \frac{4}{n} \frac{q^n}{1 - q^{2n}} \sin n\pi\varphi_{1D} \qquad (48)$$

The general solution becomes

$$\delta = \pi \frac{K}{K'} \left(\varphi_{1D} - \frac{\theta}{\pi}\right) \psi_1 + 4 \sum_{n=1}^{\infty} \frac{q^n}{n(1 - q^{2n})} \sin n\pi\varphi_{1D} \sinh n\pi\psi_1 \cos n\pi\varphi_1 \qquad (49)$$

By inspection the harmonic conjugate

$$\ln \frac{V}{U} = -\pi \frac{K}{K'} \left(\varphi_{1D} - \frac{\theta}{\pi}\right) \varphi_1 - 4 \sum_{n=1}^{\infty} \frac{q^n}{n(1 - q^{2n})} \sin n\pi\varphi_{1D} \cosh n\pi\psi_1 \sin n\pi\varphi_1 \qquad (50)$$

On line AFE ln V/U is 0. On line BC, however, ln V/U $\neq$ 0 unless A_o = 0; in other words

$$\varphi_{1D} = \frac{\theta}{\pi}$$

This relationship means that the location of point D in the w_1-plane is related by the magnitude of θ.

By inspection the logarithmic complex velocity

$$\Omega = -4 \sum_{n=1}^{\infty} \frac{q^n}{n(1 - q^{2n})} \sin n\pi\varphi_{1D} \sin n\pi w_1 \qquad (51)$$

The infinite series can be expressed in terms of elliptic functions, Hancock (7), such that

$$\Omega = 2\pi \left[Kw_1, K\varphi_{1D}\right] - 2Kw_1 Z \left[K\varphi_{1D}\right] \qquad (52)$$

21

in which Π is Legendre's incomplete elliptic integral of the third kind and Z is the Jacobian zeta function. For purposes of numerical computation it is more suitable to relate Π and Z to Jacobi's theta functions; from **Hancock**

$$\Omega = \ln \frac{\Theta\left[Kw_1 - K\varphi_{1D}\right]}{\Theta\left[Kw_1 + K\varphi_{1D}\right]}$$

Written for inclusion in equation (24)

$$e^{-\Omega} = \frac{\Theta\left[Kw_1 + K\varphi_{1D}\right]}{\Theta\left[Kw_1 - K\varphi_{1D}\right]} \tag{53}$$

For a curved boundary on EDC $g(\varphi_1)$ is not a constant and

$$A_n = \frac{2}{n} \sin n\pi\varphi_{1D} - 4 \frac{q^n}{1 - q^{2n}} \int_0^1 g(\varphi_1) \cos n\pi\varphi_1 d\varphi_1 \tag{54}$$

The first term is identical to that for the flat-plate solution except that φ_{1D} will vary, depending on the expression $g(\varphi_1)$ and the requirement that $A_0 = 0$ (in order that $\ln V/U = 0$ on BC). The expression for $e^{-\Omega}$ can be written for a curved boundary as

$$e^{-\Omega} = \frac{\Theta\left[Kw_1 + K\varphi_{1D}\right]}{\Theta\left[Kw_1 - K\varphi_{1D}\right]} \ G(w_1) \tag{55}$$

in which

$$G(w_1) = \exp\left\{ \sum_{n=1}^{\infty} A'_n \sin n\pi w_1 \right\} \tag{56}$$

and, in which $A'_n \sinh (n\pi K'/K) = -2 \int_0^1 g(\varphi_1) \cos n\pi\varphi_1 d\varphi_1$

For expedient calculation of the Jacobian elliptic functions in the expression for dw/dw_1 the relationships between the Jacobian elliptic functions and Jacobi's eta and theta functions will be used. From Byrd and Friedman (5)

$$sn(Kw_1) = \frac{H(Kw_1)}{\sqrt{k}\ \Theta\ (Kw_1)}\ , \tag{57a}$$

$$cn(Kw_1) = \sqrt{\frac{k'}{k}}\ \frac{H_1(Kw_1)}{\Theta\ (Kw_1)}\ , \tag{57b}$$

and

$$dn(Kw_1) = \sqrt{k'}\ \frac{\Theta_1(Kw_1)}{\Theta\ (Kw_1)}\ . \tag{57c}$$

The final expression for dz

$$d[\frac{Z}{D}] = \frac{2}{\pi}\ kK\ \frac{a}{b}\left\{\left[\frac{bk\Theta^2(Kw_1) - H^2(Kw_1)}{ak\Theta^2(Kw_1) + H^2(Kw_1)}\right]\left[\frac{\Theta(Kw_1)\ \Theta_1(Kw_1)}{H(Kw_1)\ H_1(Kw_1)}\right]\right.$$
$$\left.\left[\frac{\Theta(Kw_1 + K\varphi_{1D})}{\Theta(Kw_1 - K\varphi_{1D})}\right]\right\}\ G(w_1)dw_1 \tag{58}$$

For the flat plate $\varphi_{1D} = \theta/\pi$ and $G(w_1) = 1$. The parameter φ_{1D} and the function $G(w_1)$ depend solely on the function $g(\varphi_1)$ describing the shape of EDC.

The three curved-boundary functions will be referred to as the sine-, cosine-, and dn-functions.

For the sine-function

$$g(\varphi_1) = \frac{\pi}{\sigma}\left[\lambda - \sin\frac{\pi}{2}\ \varphi_1\right] \tag{59}$$

23

in which σ and λ are constants. The angle of the fluid leaving EDC at points E and C is

$$\delta_E = \pi(1 - \frac{\lambda}{\sigma}), \tag{60a}$$

$$\delta_C = - \frac{(\lambda - 1)}{\sigma} \pi \tag{60b}$$

The value of σ must be greater than two in order that the fluid leaves E in the second quadrant. In order that δ_C is negative, $\lambda > 1$. In order that $A_o = 0$

$$\varphi_{1D} = \frac{1}{\sigma} [\lambda - \frac{2}{\pi}]$$

The coefficient

$$A_n' = - \frac{8}{\sigma} \frac{q^n}{(4n^2 - 1)(1 - q^{2n})}$$

and

$$G(w_1) = \exp \left\{ - \frac{8}{\sigma} \sum_{n=1}^{\infty} \frac{q^n}{(4n^2 - 1)(1 - q^{2n})} \sin n\pi w_1 \right\} \tag{61}$$

For the cosine-function

$$g(\varphi_1) = \frac{\pi}{\sigma} [\lambda + \cos \pi\varphi_1] \; ; \; \lambda > 1, \; \sigma > 4$$

The angles

$$\delta_E = \pi \left[1 - \frac{(\lambda + 1)}{\sigma} \right] , \tag{62a}$$

24

and

$$\delta_C = - \frac{(\lambda - 1)}{\sigma} \pi \qquad (62b)$$

The location of D in w_1-plane

$$\varphi_{1D} = \frac{\lambda}{\sigma}$$

The curved-boundary function

$$G(w_1) = \exp\left\{ - \frac{2\pi}{\sigma} \frac{q}{1 - q^2} \sin \pi w_1 \right\} \qquad (63)$$

Finally, for the dn-function

$$g(\varphi_1) = \frac{\pi}{\sigma} dn(Kw_1) ; \quad \sigma > 2$$

The angles

$$\delta_E = \pi \left(\frac{\sigma - 1}{\sigma}\right), \qquad (64a)$$

and

$$\varphi_C = - \frac{\pi}{\sigma} k' \qquad (64b)$$

For point D

$$\varphi_{1D} = \frac{\pi}{2K\sigma}$$

The expression for the effect of curvature

$$G(w_1) = \exp\left\{ -\frac{\pi}{\sigma}\left[\frac{\Theta'\left(\dfrac{Kw_1}{2}\right)}{\Theta\left(\dfrac{Kw_1}{2}\right)} + \frac{\Theta'\left(\dfrac{Kw_1}{2} + K\right)}{\Theta\left(\dfrac{Kw_1}{2} + K\right)} \right] \right\} \qquad (65)$$

The curved-boundary function $f(\varphi_1)$ is shown in Figure 9 for the three functions. For the sine-function $\sigma = 3$ and $\lambda = 1$. For the cosine-function $\sigma = 6$ and $\lambda = 1$. For the dn-function $\sigma = 3$ and $k^2 = 0.9999$. The flat-plate condition is also displayed for $\theta = \pi/3$.

The computation of Jacobi's eta and theta functions and the numerical integration of equation (58) is greatly facilitated if the functions are expressed in terms of infinite series, as outlined in Appendix B. A computer program for the numerical evaluation of the parameters involved in the theory is included as Appendix C. The results of the theory are discussed in the following.

DISCUSSION OF RESULTS

The results of this investigation are discussed with reference to the force exerted on the tire surface by the water and the pressure distribution on the pavement. The force on the tire can be resolved into its vertical and horizontal components, commonly called lift and drag, respectively. When the lift force equals the weight force transmitted to the wheel, hydroplaning will occur. The amount the tire lifts off the pavement surface depends on the tire shape, water depth, and the speed of the vehicle. There will obviously be an equilibrium position of the tire for each speed greater than that required for incipient hydroplaning. The lift coefficients from this study are compared with experimental results of Horne and Dreher in the following. A comparison is also made between the theoretical and measured pressure distribution on the pavement. The shape of the planing surface selected to simulate the wetted portion of a hydroplaning tire is discussed first.

Resulting Shape of Planing Surface - The shape of the curved surface simulating the tire is assumed in the theoretical development. Three different functions were chosen to produce shapes resembling the wetted portion of a tire. They are known as the sine-, cosine-, and dn-functions. The least satisfactory is the dn-function as it results in very slight curvature and too great a clearance between tire and pavement. The cosine-function results in a tire having con-siderable more curvature on EDC, but is not entirely adequate. The resulting shape of the tire, the initial water depth, and the clearance between the tire and pavement are most realistic when the sine-function is used. For the sine-function the tire shapes and flow patterns that appear to more closely simulate tire hydroplaning at various degrees are shown in Figures 10 through 14. One

27

pattern resulting from the cosine-function is shown in Figure 15. The physical
variables for each situation presented are the clearance in terms of the water
depth, h/D, the angle of the water leaving the tire at points E and C, the length
of the tire surface referenced to the water depth, ℓ/D, and, to some degree, a
change in tire shape. For the results presented the ration ℓ/D is greater than
4; the ratio h/D was chosen to be less than $1/2$; the angle at E was varied from
109.3° to 150°; and the angle at C was maintained greater than -9°. The shape
of the tire is seen to change only slightly as the elliptic modulus, k, is
varied. The theory does not include the unwetted portion of the tire; that is,
above point E. Hence all resulting shapes that showed the water jet leaving
point E and curving severly clockwise towards the imagined continuation of the
tire shape E were discarded.

The resulting shapes do resemble the water-contact area of a hydroplaning
tire. Figure 10 simulates essentially incipient hydroplaning as the water
leaving under the tire constitutes a small fraction of the initial depth.
Figures 11 through 13 show the flow pattern as the hydroplaning becomes more and
more severe. For Figure 14 the angles δ_C and δ_E are different than those for
the shapes shown in Figures 10 through 13.

Comparison of Lift Forces - The hydrodynamic lift force can always be related
to a lift coefficient through equation (2)

$$F_L = C_L A \frac{\rho U^2}{2}$$

As mentioned in the section concerning the various fluid-property effects,
Horne and Dreher represented the characteristic area, A, by the static foot-
print area and U by the velocity of the vehicle at the condition of incipient

hydroplaning. To an approximation, then, the load on the wheel can be equated to p_i A, in which p_i is the tire inflation pressure. The lift coefficient associated with incipient hydroplaning can be computed from test results from

$$C_{Li} = \frac{p_i}{\rho U^2/2}$$

As a result of this definition of the characteristic area there is only one value of the lift coefficient associated with incipient hydroplaning of a given tire. Below incipient hydroplaning speeds $C_L > C_{Li}$. Above incipient hydroplaning speeds $C_L < C_{Li}$. It is not apparent, however, that C_{Li} should be a constant for all tire pressures and water depths as the flow pattern obviously depends on these quantities. In any case Horne and Dreher found that, from tests covering a range of tire-inflation pressures from 24 psi to 150 psi, of vehicle speeds from 45 mph to 120 mph, and of vehicle loads from 125 lb to 22,000 lb, $C_{Li} \simeq 0.7$. Their tests covered values of water depths greater than those associated with the viscous phenomenon (lubrication).

In comparing theoretical results with those of Horne and Dreher there is a question as to what characteristic area to use. Since the theory is based on two-dimensional flow only one dimension needs to be chosen for the characteristic area, A. The water depth, D, is not chosen as it does not appear to be a significant variable in the results of Horne and Dreher. It is believed that the area of the tire in contact with the water would most closely represent the tire footprint area used in the analysis of the experimental results. The area A per unit width of tire is thence chosen to be ℓ, the total length of the planing plate. The lift coefficient for hydroplaning is defined by

$$C_L = \frac{F_L}{\rho \ell U^2/2}$$

29

in which F_L in this case is the force per unit width of tire. The lift coefficient should decrease for a given tire shape and water depth as the clearance, h, is increased. Physically this means that as the speed of the vehicle is increased there is a subsequent increase in the clearance as less fluid has to have its momentum changed to provide the same lift force. Each of the tire shapes and clearances presented here simulate an assumed equilibrium condition; that is, the tire is held at its particular clearance by a balance of lift force and vehicle load for that water depth, tire-inflation pressure, and vehicle speed. It should be noted that the tire-inflation pressure is only indirectly involved in the theory by this concept of equilibrium condition.

The flow pattern depicted by the shape of Figure 10 is believed to most closely simulate incipient hydroplaning as there is a minimal amount of water flowing under the tire. The theoretical lift coefficient of approximately 0.8 can only be compared to the experimental one of 0.7 if the characteristic areas in equation (2) are identical. It is believed that the area based on the wetted length of the plate in the theory is not unlike the static footprint area used in the analysis of the experimental results for the following reason. As shown by Horne and Dreher the actual effective area of the pavement that is subject to significant water pressures is a vertical projection of the static footprint area. To an approximation, then, the effective wetted area of the tire is the static footprint area. If the wetted area of the curved surface incorporated in the theory can be assumed to be similar to the static footprint area then the lift coefficients are similarly defined for theory and experiment. If this similarity actually exists then it is not surprising that the lift coefficient from theory (0.8) is greater than that from experiment (0.7) as the three-dimensional effect precludes a uniform pressure distribution completely

across the tire.

Figures 11 through 13 are considered to simulate a tire undergoing total hydroplaning. As the clearance between the tire and pavement is increased the lift coefficient is seen to decrease, meaning that, for the same wheel load, the vehicle speed necessarily has to be greater than that for smaller clearances. In actuality the clearance automatically becomes greater as the speed is increased.

Drag Force - The hydrodynamic drag force is defined by

$$F_D = C_D A \frac{\rho U^2}{2}$$

in which C_D is a drag coefficient, depending on the same quantities as the lift coefficient, C_L. For the theoretical analysis the drag force is per unit width of tire and A is defined as the planing surface width, ℓ, times the unit width. Values of C_D are indicated in Figures 10 through 15 for the respective planing surfaces. As the clearance increases for the planing surface the drag coefficient decreases as less fluid has its momentum changed. No attempt is made to compare the theoretical values of C_D with experiment as the characteristic area used by Horne et al (9) for the drag equation differs from the area defined here.

Pressure Distribution on the Pavement - The distribution of the water pressure on the pavement can be computed from Bernoulli's equation. It is more significant to represent the pressure distribution in terms of a pressure coefficient

$$C_p = \frac{p - p_O}{\rho U^2/2} = 1 - \left(\frac{V}{U}\right)^2 \tag{66}$$

Where the pressure is atmospheric $C_p = 0$; whereas at a stagnation point $C_p = 1$. Since the only stagnation point in the flow is on the planing surface $C_p < 1$ on the pavement. For the condition of incipient hydroplaning C_p will approach unity somewhere on the pavement.

The theoretical pressure distribution on the pavement is shown in Figure 16 for a typical planing surface. The corresponding experimental pressure distribution, from Horne (8) is shown as a comparison in Figure 17. In both illustrations the horizontal coordinate is in terms of the water depth, or x/D. The marked similarity between theory and experiment further indicates that the planing surface in effect essentially simulates a tire undergoing incipient to total hydroplaning. Figures 16 and 17 were not superposed as there is actually no way to reference the horizontal coordinates of the theoretical surface to those of the actual tire. The maximum value of $C_p = 0.91$ from experiment corresponding to a maximum value of $C_p = 0.99$ from theory indicates that the tire actually had a greater clearance than the planing surface displayed in Figure 16. The planing surfaces of Figures 11, 12, and 13, having greater values of the clearance, h/D, will possess maximum values of C_p on the pavement less than 0.99. The negative pressure in front of the tire in Figure 17 can not be explained by the theory.

CONCLUSIONS AND RECOMMENDATIONS

The object of this study was to develop a theory to demonstrate the phenomenon of pneumatic tire hydroplaning from the standpoint of hydrodynamics. The strength of any theory rests in its comparison with experimental results. It is concluded that the planing surface resulting from the theory exhibits similar hydrodynamics behavior as a hydroplaning pneumatic tire as (1) the lift force from theory results in $C_L = 0.8$ at incipient hydroplaning compared with $C_L = 0.7$ from experiment, and (2) the theoretical pressure distribution on the pavement (runway) is very similar in shape to the measured pressure distribution. It is also concluded that, for moderate water depths and grooved tires, the lift coefficient for incipient hydroplaning is essentially a constant. Moreover, the assumption of an ideal fluid for tire hydroplaning is justified except for the extreme case of smooth tires and/or thin films of water on the pavement.

For future studies it is recommended that the elasticity of the tire as well as three-dimensional hydrodynamic effects be considered.

BIBLIOGRAPHY

1. Horne, Walter B. and Robert C. Dreher, "Phenomena of Pneumatic Tire Hydroplaning," NASA TN D-2056, 1963, p. 52.

2. Rouse, H., Elementary Mechanics of Fluids, John Wiley and Sons, New York, 1946.

3. Churchill, R. V., Complex Variables and Applications, McGraw-Hill, New York, 1960.

4. Bowman, F., Introduction to Elliptic Functions, Dover Publications, New York, 1961.

5. Byrd, P. F. and Friedman, M. D., Handbook of Elliptic Integrals for Engineers and Physicists, Springer-Verlag, Berlin, 1954.

6. Churchill, R. V., Fourier Series and Boundary Value Problems, McGraw-Hill, New York, 1941.

7. Hancock, H., Theory of Elliptic Functions, John Wiley and Sons, New York, 1910.

8. Horne, W. B. (private communication).

9. Horne, W. B., Joyner, U. T., and T. J. W. Leland, "Studies of the Retardation Force Developed on an Aircraft Tire Rolling in Slush or Water," NASA TN D-552, September 1960, p. 29.

APPENDIX A
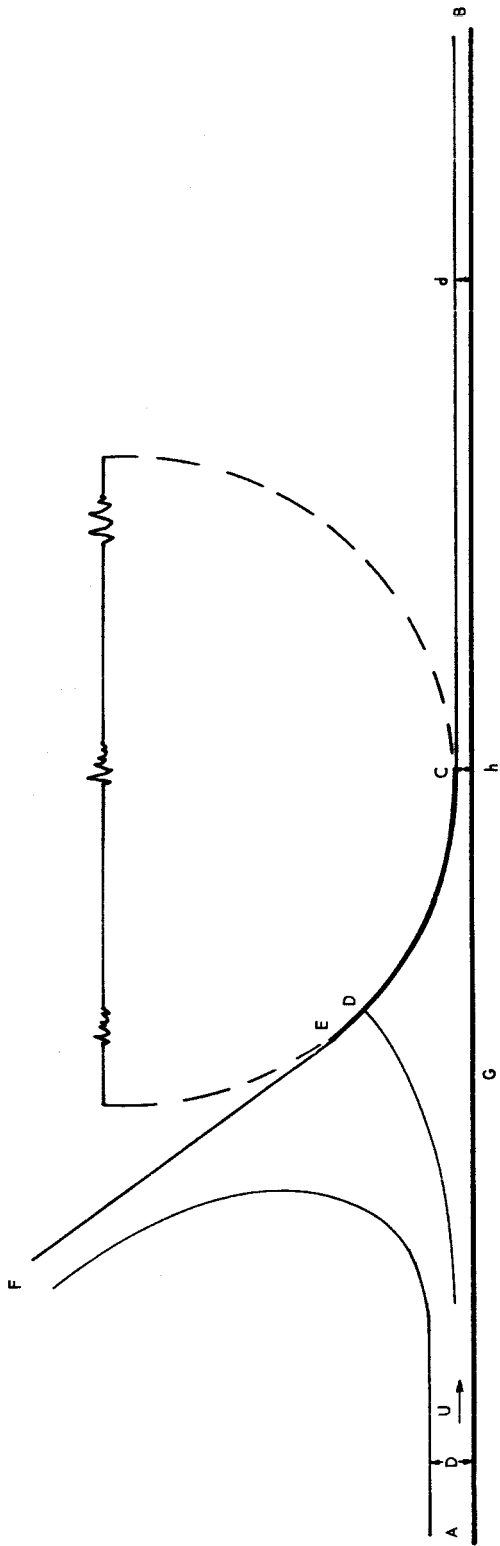
Figure 1. z-, or Physical, Plane.
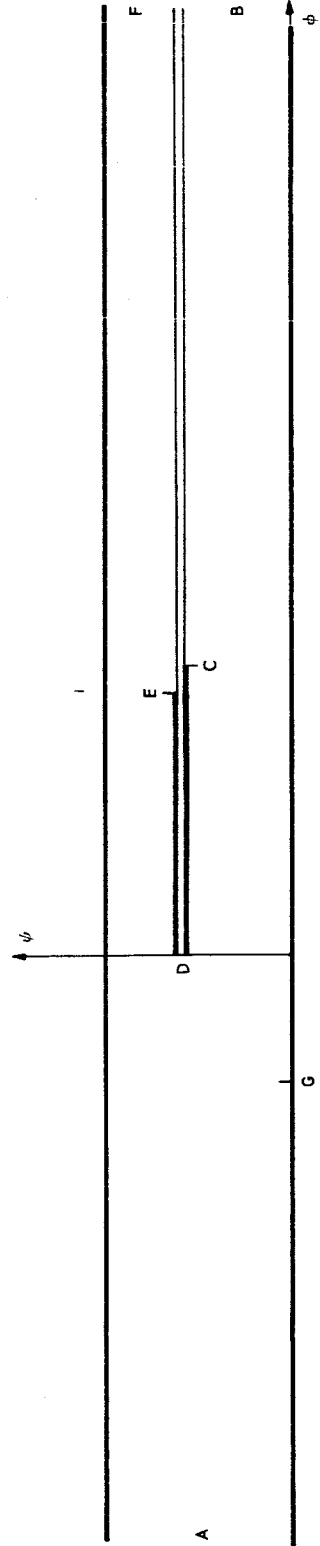
Figure 2. w-, or Complex-Potential, Plane.

36
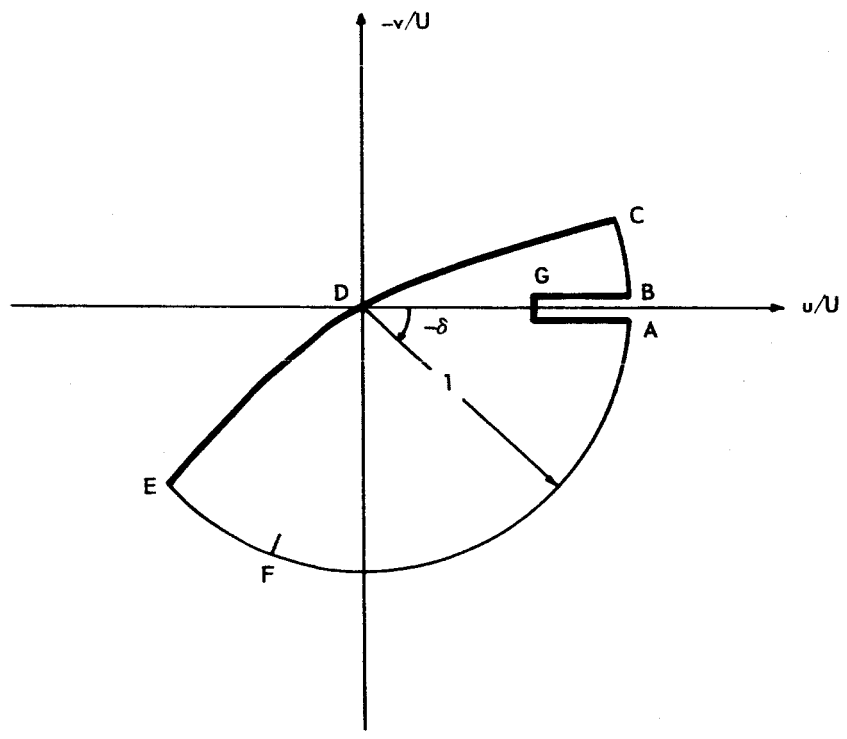
Figure 3.   ζ-, or Hodograph, Plane.
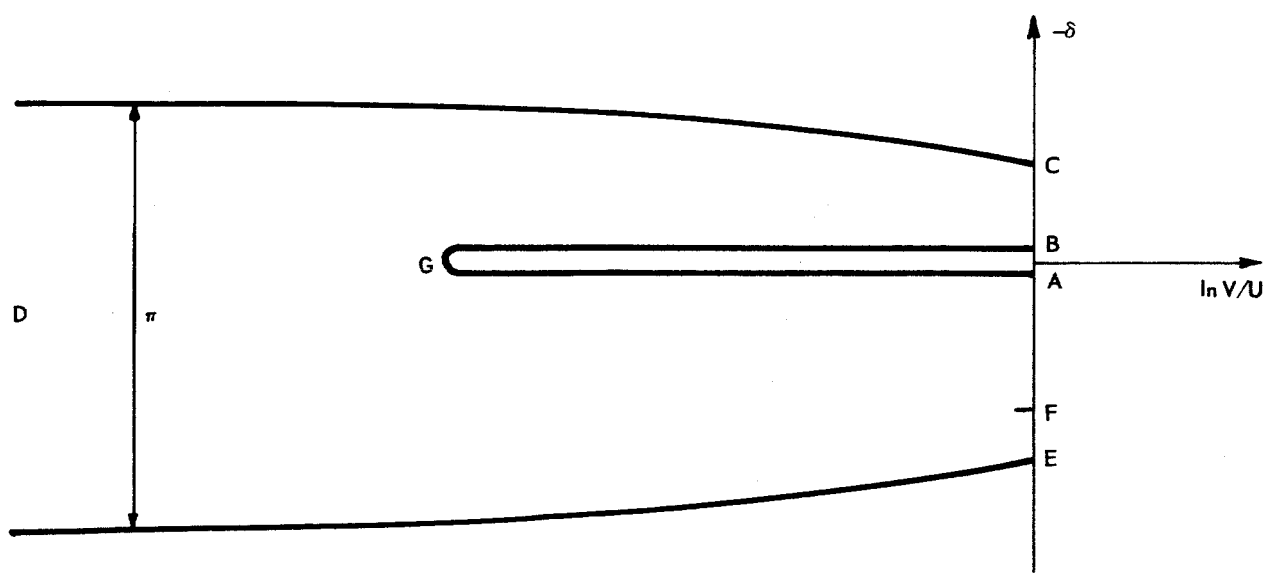
Figure 4.   Ω-, or Logarithmic Hodograph, Plane.
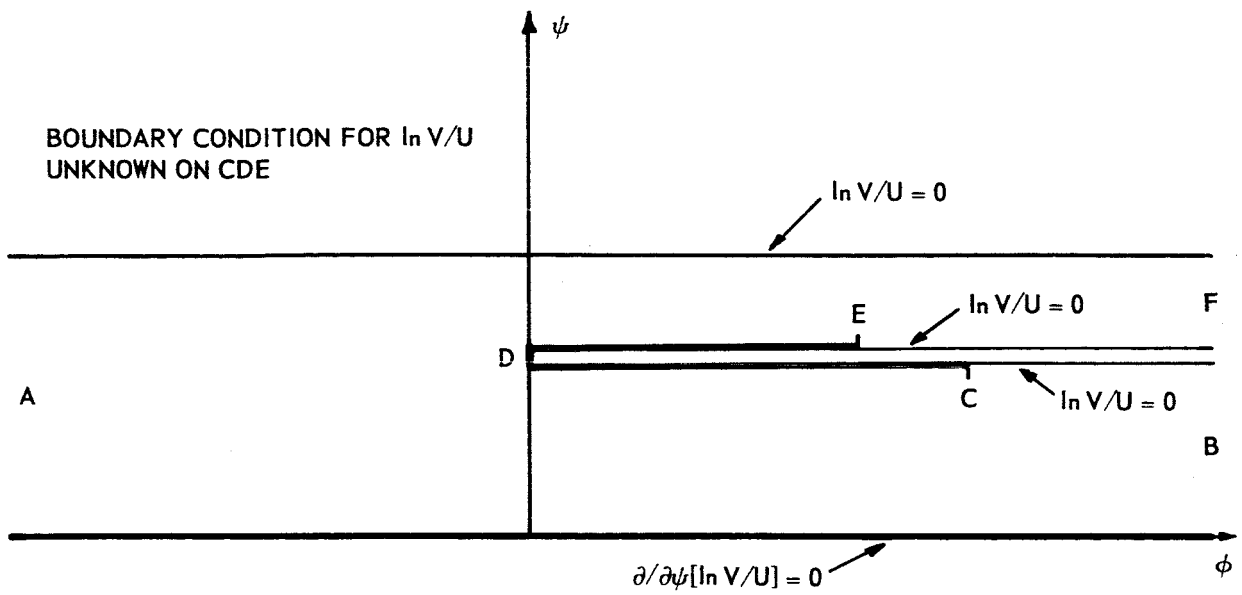
Figure 5. Boundary Conditions for ln V/U in w-Plane.
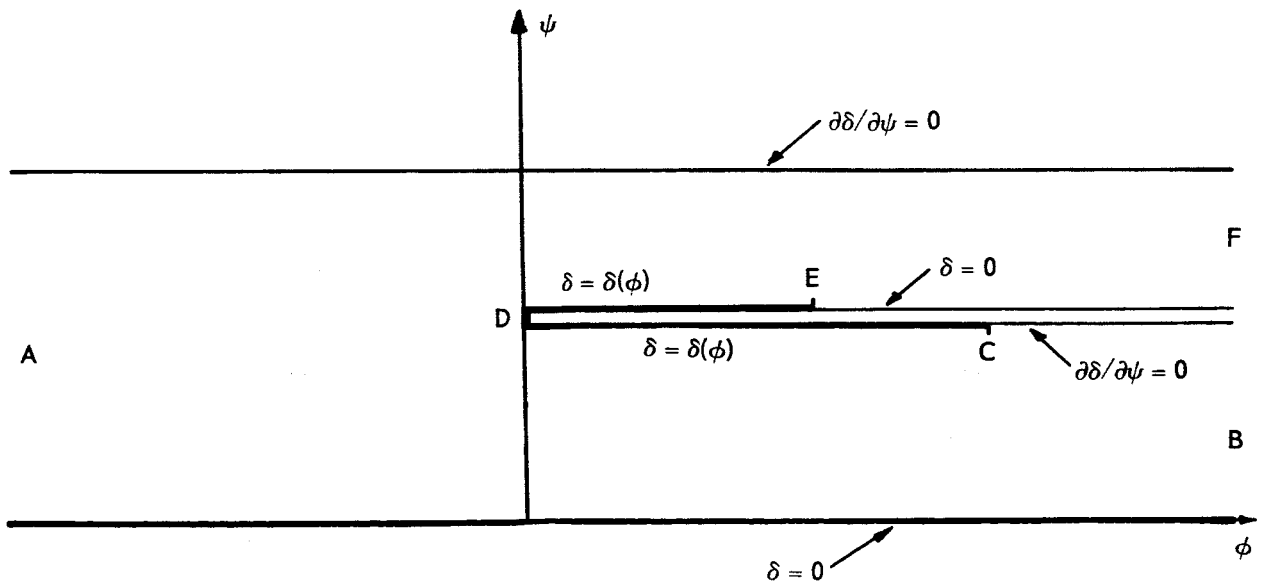
Figure 6. Boundary Conditions for δ in w-Plane.

38
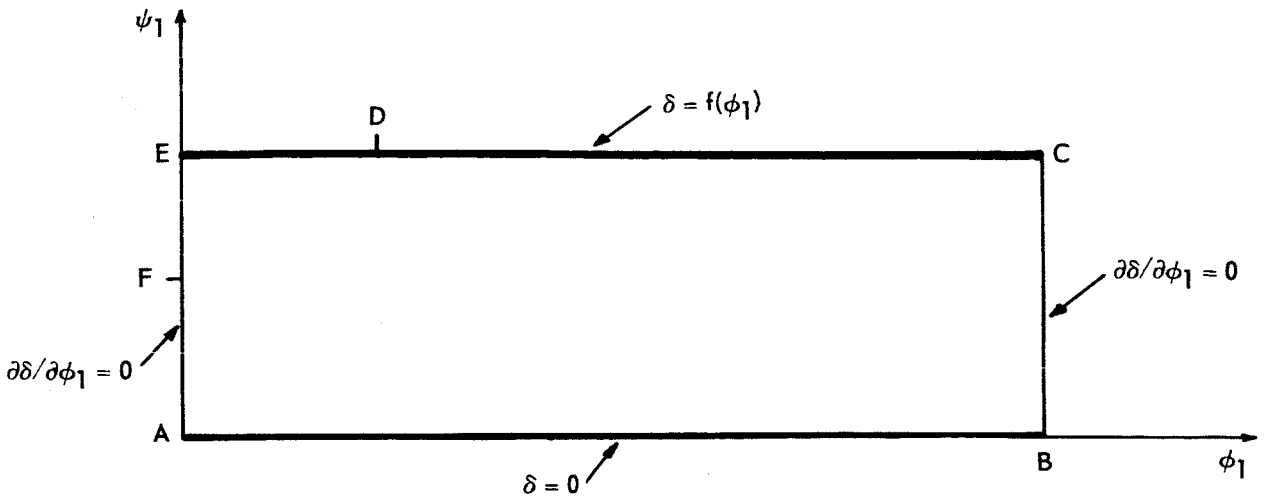
Figure 7. w_1-Plane.

Figure 8. t-, or Intermediate, Plane.
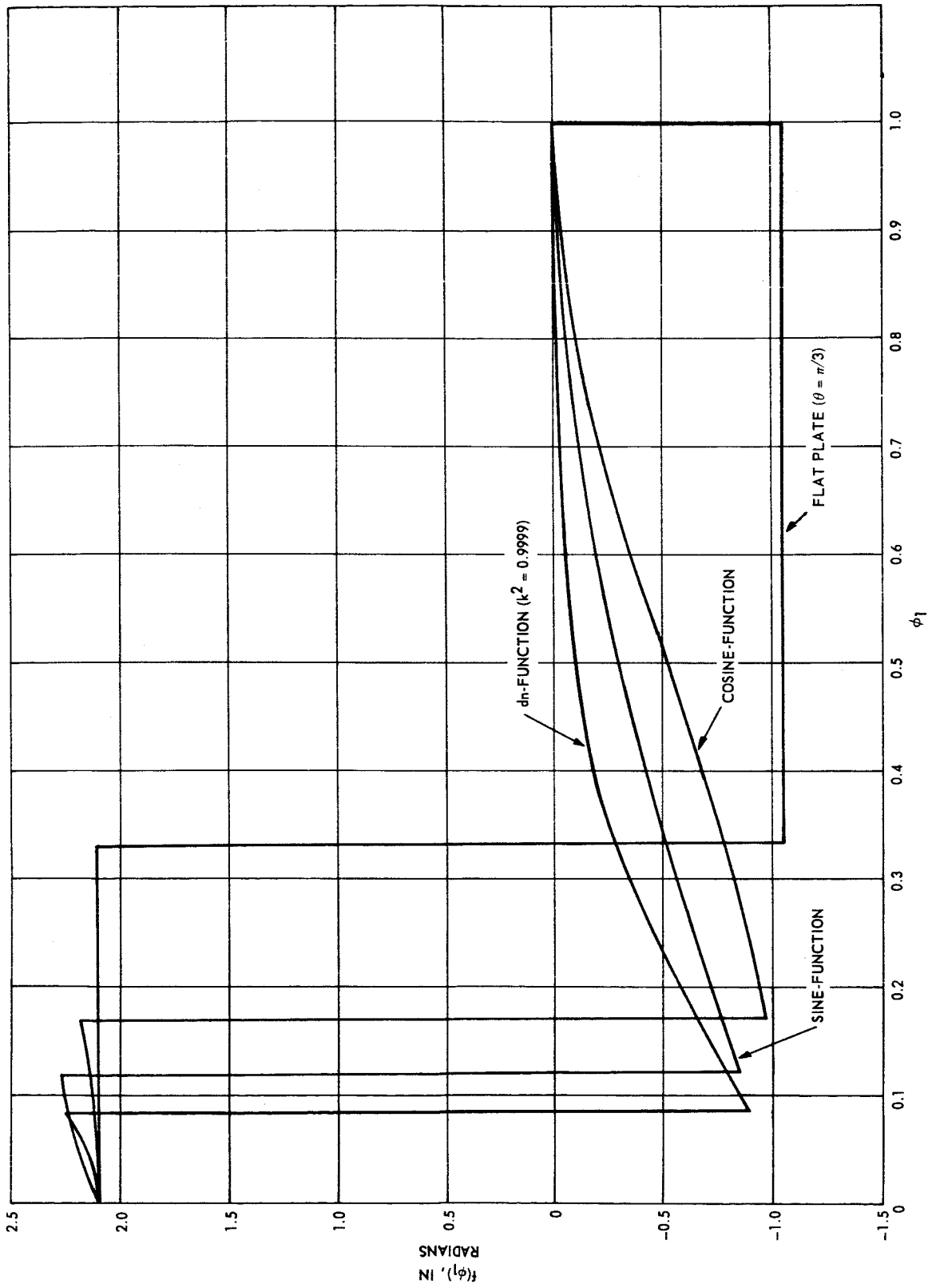
Figure 9. Relationship for Function, $f(\phi_1)$, Describing Planing Surface.

40
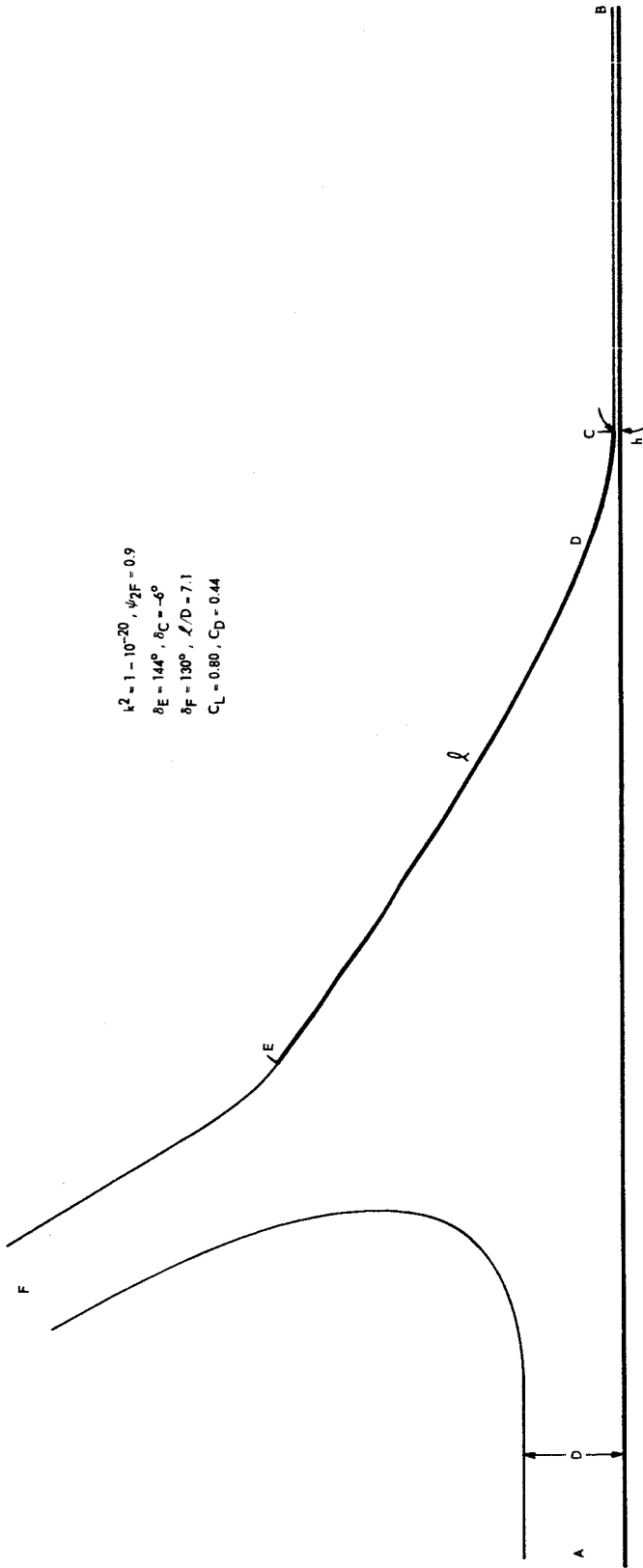
Figure 10. Hydroplaning (Incipient) for Curved Surface Described by Sine-Function ($h/D = 0.04$).

$k^2 = 1 - 10^{-20}$, $\psi_{2F} = 0.9$

$\delta_E = 144°$, $\delta_C = -6°$

$\delta_F = 130°$, $\ell/D = 7.1$

$C_L = 0.80$, $C_D = 0.44$

$k^2 = 1 - 10^{-14}$, $\psi_{2F} = 0.9$

$\delta_E = 144°$, $\delta = -6°$

$\delta_F = 129°$, $\ell/D = 7.0$

$C_L = 0.79$, $C_D = 0.40$
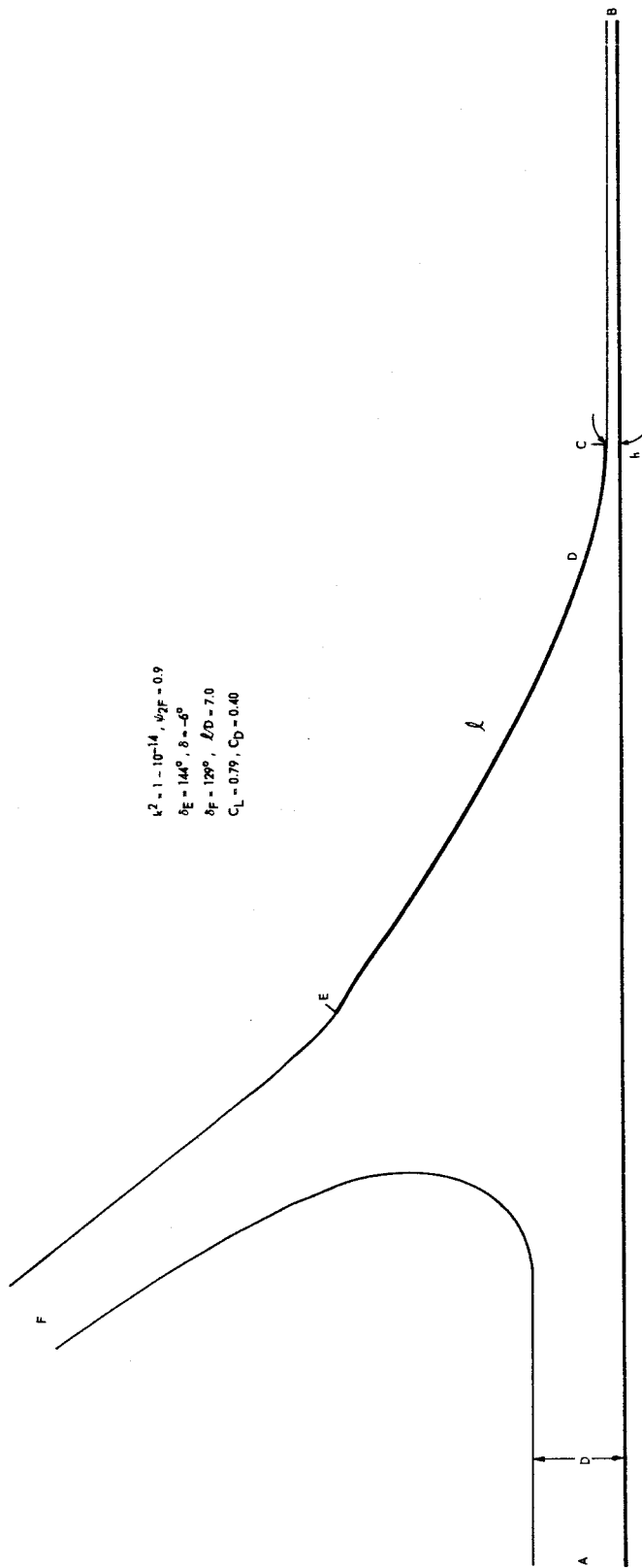
Figure 11. Hydroplaning for Curved Surface Described by Sine-Function ($h/D = 0.14$).

$k^2 = 1 - 10^{-12}$, $\psi_{2F} = 0.9$

$\delta_E = 144°$, $\delta_C = -6°$

$\delta_F = 138°$, $\ell/D = 6.9$

$C_L = 0.76$, $C_D = 0.38$
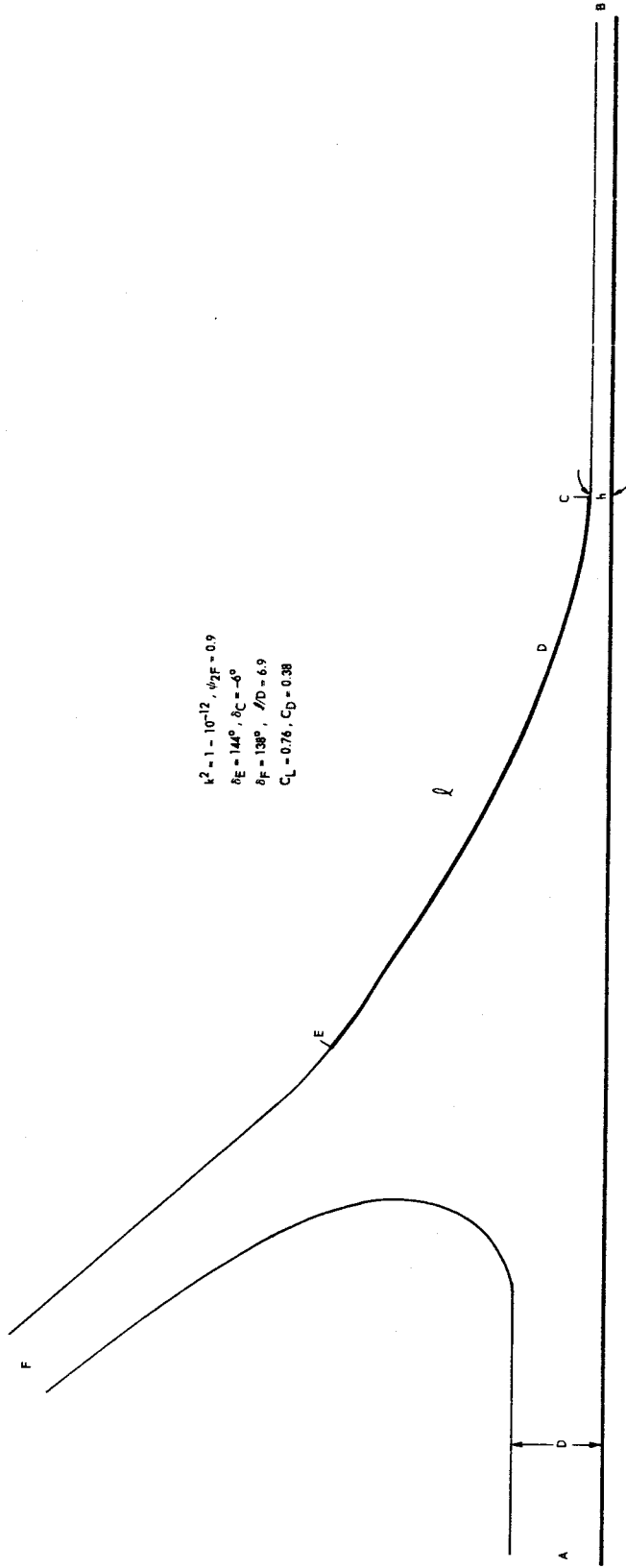
Figure 12. Hydroplaning for Curved Surface Described by Sine-Function (h/D = 0.21).

43

$k^2 = 1 - 10^{-8}$, $\psi_{2F} = 0.9$

$\delta_E = 144°$, $\delta_C = -6°$

$\delta_F = 135°$, $l/D = 5.9$

$C_L = 0.67$, $C_D = 0.31$
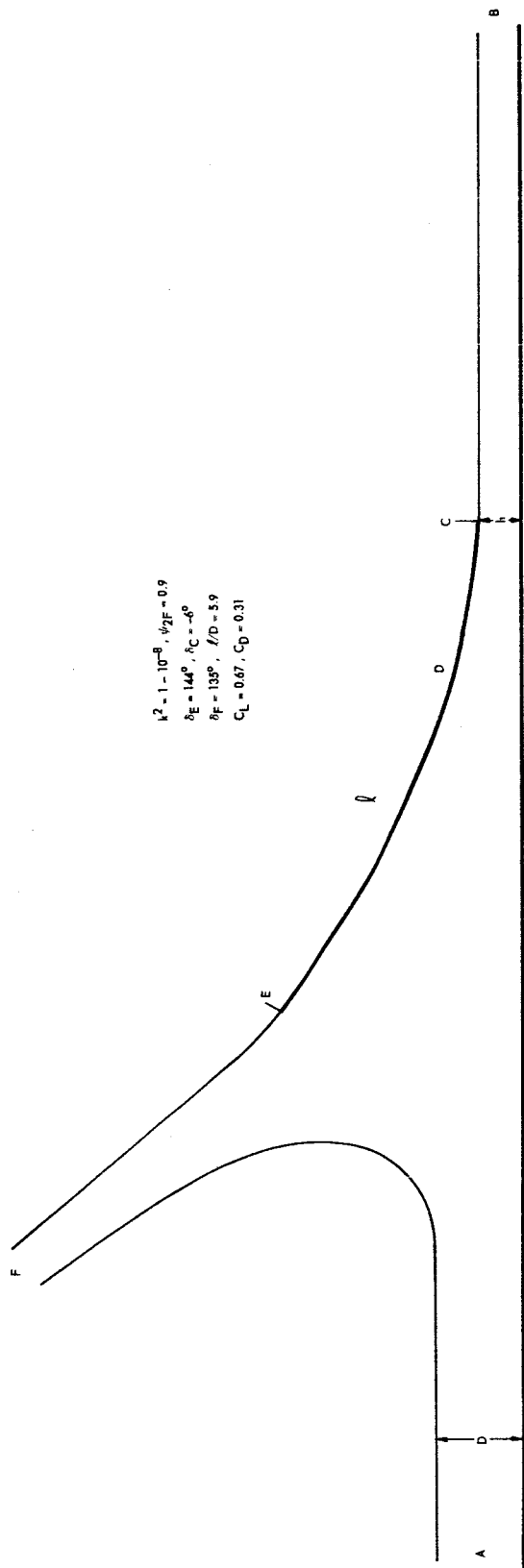
Figure 13. Hydroplaning for Curved Surface Described by Sine–Function (h/D = 0.43).

44

$k^2 = 1 - 10^{-10}, \; \psi_{2F} = 0.9$
$\delta_E = 128°, \; \delta_C = -9°$
$\delta_F = 114°, \; \ell/D = 4.7$
$C_L = 0.62, \; C_D = 0.53$
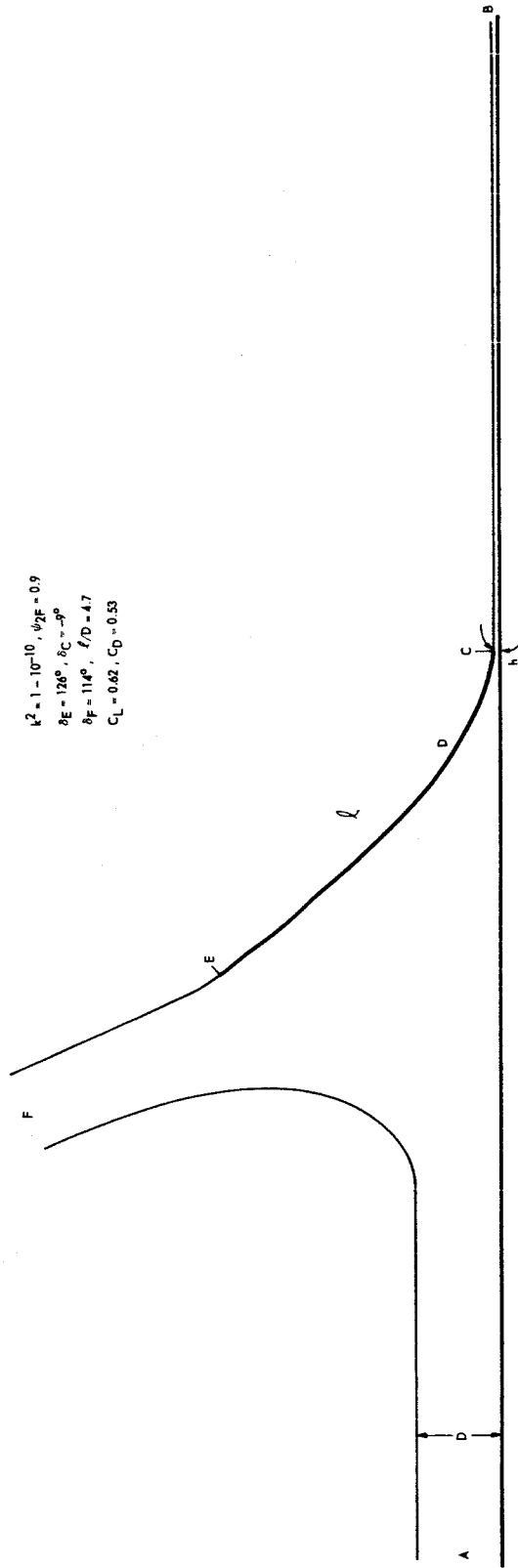
Figure 14. Hydroplaning for Curved Surface Described by Sine-Function (h/D = 0.11).

$k^2 = 1 - 10^{-10}$, $\psi_{2F} = 0.9$

$\delta_E = 150°$, $\delta_C = 0.2°$

$\delta_F = 129°$, $\ell/D = 6.6$

$C_L = 0.66$, $C_D = 0.33$
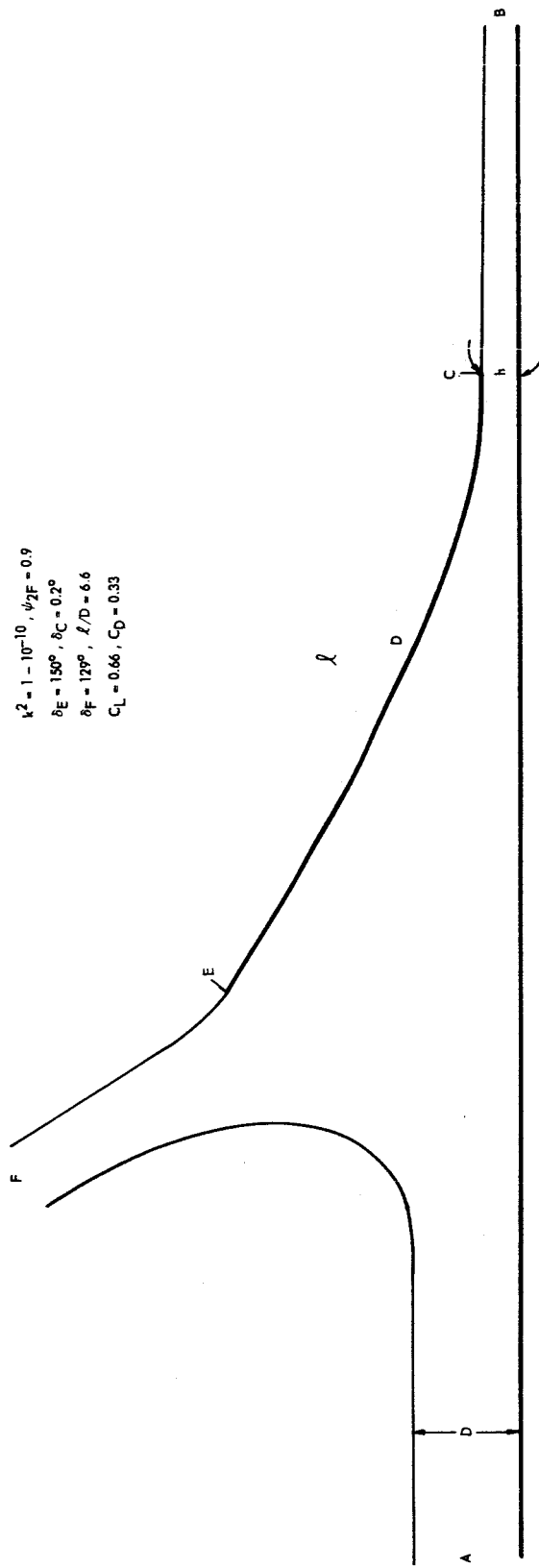
Figure 15. Hydroplaning for Curved Surface Described by Cosine-Function (h/D = 0.36).

$k^2 = 1 - 10^{-14}, \psi_{2F} = 0.9$
$\delta_E = 144°, \delta_C = -6°$
$l/D = 7.2, \delta_F = 31°$

$C_L = 0.76, C_D = 0.39$
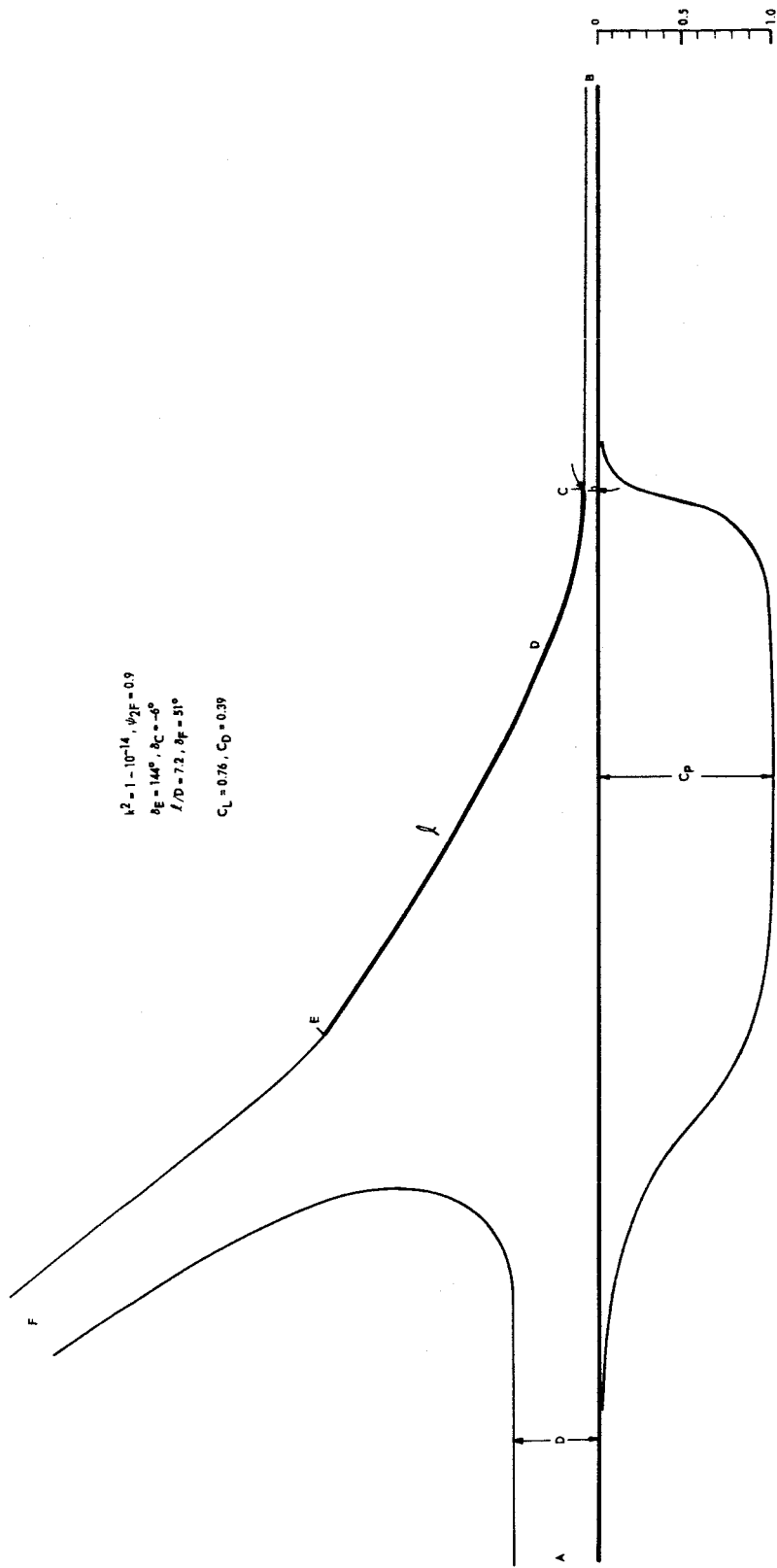
Figure 16. Pressure Distribution on Runway from Theory for Sine-Function (h/D = 0.14).

TRAILING EDGE OF TIRE
UNDER STATIC
CONDITIONS

LEADING EDGE OF TIRE
UNDER STATIC
CONDITIONS
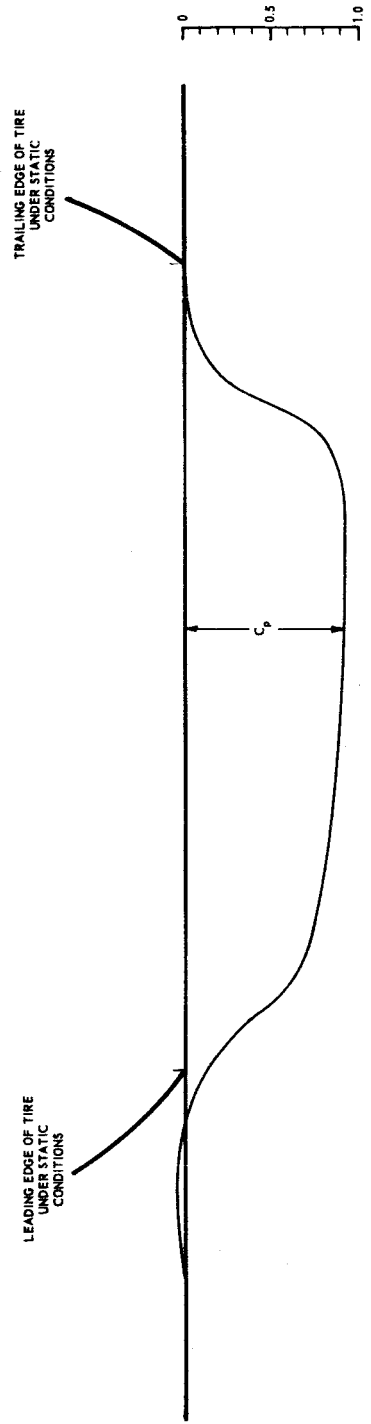
Figure 17. Pressure Distribution on Runway Under Center Groove from Experimental Results of Horne (8).

47

APPENDIX B

APPENDIX B

ELLIPTIC FUNCTIONS AND NUMERICAL TECHNIQUES OF COMPUTATION

The square of the modulus of the Jacobian elliptic functions, k^2, is regarded as the independent variable. The square of the complementary modulus

$$k'^2 = 1 - k^2 \tag{67}$$

For moderate values of k^2 Jacobi's nome can be computed from the series, Whittaker and Watson[*]

$$q = \epsilon + 2\epsilon^5 + 15\epsilon^9 + 150\epsilon^{13} + \ldots \tag{68}$$

in which

$$\epsilon = \frac{1}{2}\left[\frac{1 - \sqrt{k'}}{1 + \sqrt{k'}}\right] \tag{69}$$

The elliptic integral of the first kind is related to q by

$$K = \frac{\pi}{2}\left[1 + 2\sum_{n=1}^{\infty} q^{n^2}\right]^2 \tag{70}$$

And, by definition of the nome

$$K' = \frac{K}{\pi} \ln \frac{1}{q} \tag{71}$$

For values of k^2 near 1 (the largest chosen in this study was $1 - 10^{-30}$) the series for q does not converge rapidly enough. From Byrd and Friedman[**], for

---

[*] Whittaker, E. T. and G. N. Watson, <u>A Course of Modern Analysis</u>, Cambridge University Press, Cambridge, 1944.

[**] Byrd, P. F. and M. D. Friedman, <u>Handbook of Elliptic Integrals for Engineers and Physicists</u>, Springer-Verlag, Berlin, 1954.

k^2 approaching unity the elliptic parameters are best determined by

$$K = \Lambda + \frac{1}{4} k'^2 [\Lambda - 1] + \frac{9}{64} k'^4 \left[\Lambda - \frac{7}{6}\right] + \frac{25}{256} k'^6 \left[\Lambda - \frac{37}{30}\right] + \ldots \quad (72)$$

in which $\Lambda = \ln \frac{4}{k'}$,

$$K' = \frac{\pi}{2} \left[1 + \frac{1}{4} k'^2 + \frac{9}{64} k'^4 + \frac{25}{256} k'^6 + \frac{1225}{16384} k'^8 + \ldots \right], \quad (73)$$

and

$$q = \exp(-\pi K'/K) \quad (74)$$

These two series give adequate convergence for values of k^2 as large as $1 - 10^{-50}$.

The rapidly converging infinite series for the eta and theta functions, Byrd and Friedman, are suitable for numerical calculations

$$H(Kw_1) = 2 \sum_{n=1}^{\infty} (-1)^{n-1} q^{\left(n-\frac{1}{2}\right)^2} \sin\left[(n - \frac{1}{2})\pi w_1\right] \quad (75a)$$

$$H_1(Kw_1) = 2 \sum_{n=1}^{\infty} q^{\left(n-\frac{1}{2}\right)^2} \cos\left[(n - \frac{1}{2})\pi w_1\right] \quad (75b)$$

$$\Theta(Kw_1) = 1 + 2 \sum_{n=1}^{\infty} (-1)^n q^{n^2} \cos n\pi w_1 \quad (75c)$$

and

$$\Theta_1(Kw_1) = 1 + 2 \sum_{n=1}^{\infty} q^{n^2} \cos n\pi w_1 \quad (75d)$$

The location of point F in the t-plane depends on the value of the modulus,

k, and the location of F in the w_1-plane. From equation (33) and the above relations

$$a = -\frac{1}{k} \frac{H^2\left[iK\psi_{1F}\right]}{\Theta^2\left[iK\psi_{1F}\right]} \qquad (76)$$

The location of point D in the t-plane is computed from equation (34) to be

$$b = \frac{1}{k} \frac{\Theta^2(K\varphi_{1D})}{H^2(K\varphi_{1D})} \qquad (77)$$

The actual geometry of the flow pattern and the shape of the tire have to be determined by integrating equation (58). The eta and theta functions are expressed in terms of the infinite series for each line of the w_1-plane on which the equation is integrated. For each streamline in the z-plane the expression in equation (58) is reduced to its real and imaginary parts. The integration is performed by using the trapezoidal rule, Simpson's rule, or a numerical integration equation of higher order, depending on the rate of change of the integrand for the conditions specified. The shape of the tire is determined by integrating equation (58) from E to C in the w_1-plane. As an example, on line EDC

$$w_1 = \varphi_1 + i \frac{K'}{K}$$

and

$$dw_1 = d\varphi_1$$

The function $\Theta(Kw_1)$ on EDC is evaluated from

$$\Theta\left[(Kw_1)\right]_{EDC} = 1 + \sum_{n=1}^{\infty} (-n)^n q^{n^2} (q^{-n} + q^n) \cos n\pi\varphi_1$$

$$-i \sum_{n=1}^{\infty} (-1)^n q^{n^2} (q^{-n} - q^n) \sin n\pi\varphi_1$$

(78)

The other functions in equation (58) are evaluated similarly. Caution has to be taken at the singular point D. The integrand of equation (58) is indeterminate at D. By using L'Hospital's rule the integrand is found to be finite. The shape of the streamlines AFE and BC can also be determined by numerical integration of equation (58) along the respective lines in the w_1-plane.

The pressure distribution on the tire and the runway can be determined from equation (12). The total force on the tire can be determined by integrating the pressure distribution over its surface. The lift coefficient

$$C_L = \frac{\int_A C_p d\left(\frac{x}{D}\right)}{\frac{\ell}{D}} ,$$

and the drag coefficient

$$C_D = \frac{\int_A C_p d\left(\frac{y}{D}\right)}{\frac{\ell}{D}}$$

in which C_p is the pressure coefficient, defined as

$$C_p = 1 - \left(\frac{V}{U}\right)^2$$

The drag coefficient can also be computed (as a check) from a simple momentum analysis to be

$$C_D = \frac{2\left[1 - \frac{d}{D}\right]\left[1 - \cos \delta_F\right]}{\frac{\ell}{D}}$$

in which δ_F is the angle that the jet leaving the tire at E finally makes at F with the positive x-direction. The angle δ_F is computed from equation (55). The water depth at d is computed from equation (27)

$$\frac{d}{D} = \frac{a}{b}\frac{b - 1}{1 + a}$$

The clearance that the trailing edge of the surface makes with the pavement, h, is computed by integrating equation (58) from B to C in terms of the vertical coordinate, y.

The pressure distribution on the pavement is computed from equations (55) and (66). The coordinates on line AB are referenced to point C (or E) by integrating from a point near B on BC toward C. By integrating from a point near B on AB having the same value of the velocity potential, φ, as that at the corresponding point on BC the pressure distribution on AB can be referenced to CDE.

The parameters in the theory that may be varied for each of the assumed curved-surface functions are the modulus, k, the location of F in the w_1-plane, ψ_{1F}, and the parameters describing the curved-boundary function, σ and λ. Realistic planing surfaces and clearances are obtained only if the square of the modulus, k^2, is considerably greater than 0.99. Values chosen for $\psi_{2F} = (K/K')\psi_{1F}$ were 0.7 and 0.9. The chosen values of σ and λ depended on the

curved-boundary function used. The computer program utilized for evaluating

the elliptic functions and in integrating equation (58) is presented in

Appendix C.

APPENDIX C

APPENDIX C

DIGITAL COMPUTER PROGRAM

Because of the complexity of the relationships involved and the large number of infinite series appearing in the theory, a high-speed digital computer was essential in order that numerical results may be obtained. The program was written in ALGOL 60 for use by the Burroughs B-5500 of the Rich Electronic Computer Center of the Engineering Experiment Station. The coordinates of the planing surface, the pressure distribution on the runway and the gross quantities such as lift and drag coefficients and length of the planing surface are the output. The computer time required for each planing surface assumed was approximately 250 seconds.

```
BEGIN COMMENT SOLUTION FOR CURVED PLATE UNDERGOING TOTAL HYDROPLANING     ;
                USING SINE FUNCTION                                       ;
LABEL       L1,L2,L3,L4                                                   ;
INTEGER     I,J,M,N                                                       ;
REAL        PF,T,K2,K,K1,E,Q,P,PI,ST,PHI1,A,A1,A2,A3,B,B1,B2,B3,C,        ;
            C1,C2,C3,CF,CC,CKP,CK,SP,CFP,CL,CD,D,D1,D2,D3,E3,F3,SUM,
            YBCOD,LDOD,LOD,DF,S1,S2,S3,S4,S5,S6,S7,S8,S9,S10,S11,S12
            ,S13,S14,S15,S16,S17,S18,S19,S20,S21,S22,S23,S24,S25,S26
            ,S27,S28,S29,S30,S21D,VDU,YEDCOD,S3F,S4F,S7A,S7F,S8F,S3B
            ,S6B,S8A,R,RD,S18D,S19D,DELTAF,SUBTR,L,T2,T3,M3,N3,H3,G3
            ,S31,S32,S33,S34,S222 ,S35,S36,S37,X,XY,XYR,XD,Y,YD,DY,
            DX,SIGMA,S22F,S24F,S26F,S28F,XEDCOD,SUB,S22B,S23B,S25B,
            LAMBDA,SS,SSF,XBC,GW3,CW,XAB,DTBC,DTBA1,PHIB
ARRAY       FY[0:900],FX[0:900],CP [ 0:900 ] , DELTAY [ 0:900 ]           ;
            FILE OUT PRT 6 (2,15)                                         ;
            FORMAT FMT1(2F14.6///),FMTKP(10F12.6 / / / / ) ,FMT2(2F14.6
            ),
            FMT3(F10.6),FMT7(7F10.6),FMT9(9F12.6),
FMT ( "MODULUS SQUARED                Q              K           KPRIM
" , X2 / ) ,
FMTV ( X6 , "L / D        YBC / D        / D          C
C                     C    C " , X2 / ) ,
FMTK( X7 , "  A                 B  " , X2 / ) ,
FMTT( X6 , " INT-BC       INT-EC " , X2 / ) ,
FMT6(4F14.6//) ,FMT5(F10.6,2E14.5//),
FMTIME(//" PROCESS TIME " , I5, " SECONDS.         IN/OUT TIME #
" ,I5, " SECONDS " )                                                     ;
            LIST LST(LOD,YBCOD,LDOD,CC,DELTAF,CF,CFP,CL,CD,CW),           ;
            LST2( K2 , Q, CK , CKP )                                      ;
            WRITE(PRT[NO])                                                ;
COMMENT BEGIN STATEMENTS                                                  ;
            T2 +TIME(2)                                                   ;
            T3 +TIME(3)                                                   ;
            PI+3.14159265                                                 ;
            LAMBDA + 1.02                                                 ;
            SIGMA + 6                                                     ;
            C + PI / SIGMA                                                ;
```

```
COMMENT     T ← C×(LAMBDA - (2/PI))                              ;
            M← 20                                                ;
            ST ← 0.0125                                          ;
            R ← 0.0125                                           ;
            WRITE ( PRT , FMTT )                                 ;
            WRITE ( PRT , FMT1 , ST , R )                        ;
            DETERMINATION OF ELLIPTIC PARAMETERS
            FOR J ←10 STEP 8 UNTIL 18 DO
BEGIN       K1  ← SQRT((10)+(-J))                                ;
            K2  ← 1 - K1*2                                       ;
            K   ← SQRT(K2)                                       ;
            L   ← LN(4/K1)                                       ;
            CK  ← L + (1/4)×(K1*2)×(L-1) + (9/64)×(K1*4)×(L-7/6) +
                  (25/256)×(K1*6)×(L-37/30)                      ;
            CKP ← (PI/2)×(1 + (1/4)×(K1*2)+ (9/64)×(K1*4) + (25/256)×
                  (K1*6) + (1225/16384)×(K1*8) + (3969/65536)×(K1*10)) ;
            Q   ← EXP(-(PI×CKP)/CK)                              ;
            S3F←0;S4F←0;S7A←0;S9←0;S8F←0;S3B←0;S6B←0;S8A←0;SUM←0 ;
            S21D ← 0 ; S18D ← 0 ; S22B ← 0 ; S19D ← 0 ; S23B ← 0 ;
            S25B ← 0 ;
            SS ← 0 ;
            FOR N ← 1 STEP 1 UNTIL 40 DO
BEGIN       SS ← ((-1)*N)×N×(Q*(N+1))/((4×(N+2) - 1)×(1 - Q*(2×N))) + SS;
END
BEGIN       FOR N ← 1 STEP 1 UNTIL M DO
            S3B ← S3B + ( N - ( 1 / 2 ) ) × ( ( -1 ) * ( N - 1 ) ) ×
                  ( Q * ( N - ( 1 / 2 ) * 2 ) ) × SIN( N × T )   ;
            S6B ← S6B + N × ( Q * ( -1 ) ) × ( Q * ( N * 2 ) ) × SIN( N × T ) ;
            S7A ← S7A + 2 × ( -1 ) * ( N ) × ( Q * ( N * 2 ) ) ×
                  COS( N × T )                                   ;
            S8A ← S8A + ( ( -1 ) * N ) × ( Q * ( N * 2 ) ) ×
                  SIN( N × T )                                   ;
            S9 ← S9 + 2 × ( ( -1 ) * N ) × ( Q * ( N - ( 1 / 2 ) ) * 2
                  ) ) × SIN( ( N - ( 1 / 2 ) × T )
```

```
S18D ← S18D +
( Q * ( -N ) + Q * N ) × ( (-1)* N ) × ( COS ( 2×N×T )) × ( Q * ( N + 2 ) ) ×
S19D ← S19D +
( Q * ( -N ) - Q * N ) × ( (-1)* N ) × ( SIN ( 2×N×T )) × ( Q * ( N * 2 ) ) ×
S21D ← S21D + N × ( ( -1 ) * -N ) - Q * N ) × ( ( -N ) + ( N * 2 ) ) ×
              ( Q * ( -N ) - Q * N )
END
        WRITE ( PRT , FMT )
        WRITE ( PRT , FMT6 , LST2 )
        FOR PF ← 0.99 STEP 0.005 UNTIL 0.996 DO
BEGIN
        S3F ← 0 ; S4F ← 0 ; S7F ← 0 ; S8F ← 0 ;
        FOR N ← 1 STEP 1 UNTIL M DO
BEGIN
        S3F ← S3F + ( ( -1 ) * ( N - 1 ) ) × ( Q * ( ( N - ( 1 / 2 ) ) ×
                    ( 2 ) ) × ( PF × ( N - ( 1 / 2 ) ) ) ×
        S4F ← S4F + ( Q * ( N * 2 ) ) × ( -1 ) × ( N ) × ( PF × N ) ) ×
        S7F ← S7F + ( ( -1 ) * ( N ) ) × ( Q * ( N * 2 ) + ( N * 2 ) × ( PF × N ) ) × COS( N × T )
        S8F ← S8F + ( ( -1 ) * ( N ) ) × ( Q * ( N * 2 ) + ( N * 2 ) × ( PF × N ) ) × SIN( N × T )
END
        SSF ← 0 ;
        FOR N ← 1 STEP 1 UNTIL 80 DO
        SSF ← ( 4 / PI ) × ( ( Q + ( -N×PF ) - Q * ( N×PF ) ) / ( ( 4 × ( N * 2 ) - 1 ) ×
              ( Q * ( -N ) - Q * ( N ) ) ) ) + SSF
BEGIN
        A ← ( S3F * 2 ) / ( K × ( 1 + S4F ) * 2 ) )
        B ← ( ( 1 + S7A ) * 2 ) / ( K × ( S9 * 2 ) )
        WRITE ( PRT , FMTK )
        WRITE ( PRT , FMT1 , A , B )
END
COMMENT SUMMATION OF SERIES FOR INTEGRATION ON LINE BC
        I ← 0
        FOR P ← 0 STEP ST UNTIL 1 + ( ST / 2 ) DO
```

59

```
BEGIN
        S1 ← 0 ; S2 ← 0 ; S3 ← 0 ; S4 ← 0 ; S5 ← 0 ; S6 ← 0
        FOR N ← 1 STEP 1 UNTIL M DO
BEGIN
        S1 ← S1 + (Q ↑ (-N)) × (N ↑ 2) × (COS(N × P))
        S2 ← S2 + (Q ↑ (-N)) × (N ↑ 2) × (COS(N × P))
        S3 ← S3 + (Q ↑ (-N)) × (N ↑ 2) × (SIN(N × P))
        S4 ← S4 + (Q ↑ (-N)) × (COS(N × P))
        S5 ← S5 + (Q ↑ (-N)) × (SIN(N × P))
        S6 ← S6 + (Q ↑ (-N)) × (SIN(N × P))
END
        N3 ← 0 ;
        FOR N ← 1 STEP 1 UNTIL 80 DO
BEGIN
        N3 ← (-4/PI)×(((-1)↑N)×(Q↑(-N×P)) - (Q↑(-N)) - (Q↑(N)))) + N3
END
BEGIN
        IF P < ( ST / 2 ) THEN GO TO L1
        XY ← 4 × K × CKP × A × (( B × K × (( 1 + S4 )) ...
        S2 ← PI × R × (( 1 + S1) × ((( 1 + S2 ) ↑ 2 )) ...
        × ((( 1 + S5 ) ↑ 2 )) + S6 × 2 )) × COS ( C × N3 )
        FY ← XY × (( 1 + S6 )) × ( 1 + S5 ) × EXP ( C × M3 ) ...
                (( 1 / 2 )) × SIN ( C × N3 ))
        FX ← XY × (-S6 ) × ( 1 + S5 ) × EXP ( C × M3 ) ...
                (( 1 / 2 )) × COS ( C × N3 ))
END
        GO TO L2
L1 : XYR ← ( 4 × K × CKP × A × (( B × K × (( 1 + S1) ↑ 2 )) .
```

```
          S2 + 2 ) × ( 1 + S1 ) × ( 1 + S4 ) ) ) /
        ( PI × B × ( ( A × K × ( ( 1 + S1 ) + 2 ) ) + S2 + 2 ) × S2 × S3B
        × ( ( ( 1 + S5 ) + 2 ) + S6 + 2 ) )
        FY [ I ] + X↓B× ( S6B× ( 1 + S5 ) ) × COS ( C × N3 ) ) -
                (1/2)×((1 + S5)+2)×(-4/PI)×C×SS) ;

L2:     I + I + 1 ;

END
COMMENT   INTEGRATION ON LINE BC ;
          YBCOD + 0 ;
          FOR I + 0 STEP 4 UNTIL (1/ST) + (ST/2) - 4 DO

BEGIN     YBCOD + YBCOD + ((2×ST)×(7×FY[I] + 32×FY[I+1] + 12×FY[I+2]
                + 32×FY[I+3] + 7×FY[I+4]))/45 ;

END
          XBC + 0 ;
          FOR I + 1 STEP 1 UNTIL 1/ST + ST/2 - 1 DO

BEGIN     XBC + XBC +((FX[I] + FX[I+1])/2)×ST ;
          WRITE(PRT,FMT2,XBC,FX[I]) ;

END
BEGIN     LABEL L3,L4,DT,DTS ;
COMMENT   SUMMATION FOR SERIES FOR PRESSURE DISTRIBUTION ON LINE AB ;
          I + 0 ;
          R + 1/318 ;
          FOR PHI1 + 1 - R STEP -R UNTIL R/2 DO

BEGIN     S22 + 0 ; S23 + 0 ; S24 + 0 ; S25 + 0 ; S26 + 0 ; S27 + 0;
          FOR N + 1 STEP 1 UNTIL M DO

BEGIN     S22 + S22 + 2×((-1)+N)×(Q+(N+2))×COS(N×PI×PHI1) ;
          S23 + S23 + 2×((-1)+(N-1))×(Q+((N-1/2)+2))×SIN((N-1/2)×PI×
                PHI1) ;
          S24 + S24 + 2×(Q+((N-1/2)+2))×COS((N-1/2)×PI×PHI1) ;
          S25 + S25 + 2×(Q+(N+2))×COS(N×PI×PHI1) ;
          S26 + S26 + 2×((-1)+N)×(Q+(N+2))×COS(N×PI×PHI1 + N×T) ;
          S27 + S27 + 2×((-1)+N)×(Q+(N+2))×COS(N×PI×PHI1 - N×T) ;

END
```

61

```
        GW3 ← 0
        FOR N ← 1 STEP 1 UNTIL 80 DO
BEGIN
        GW3 ← GW3 + ((-8/SIGMA)×(Q+N)×SIN(N×PI×PHI1))/((4×(N+2) - 1)×
            (1 - Q+(2×N)))
END
COMMENT  DETERMINATION OF PRESSURE DISTRIBUTION ON LINE AB
        VOU ← ((1+S27)×EXP(-GW3))/(1+S26)
        CP[I] ← 1 - VOU+2
        FX[I] ← (2/PI)×K×CK×(A/B)×(((B×K×((1+S22)+2) - S23+2)×(1+S22)
        ×(1+S25)×(1+S26))/((A×K×((1+S22)+2) + S23+2)×S23×S24×
        (1+S27)))×EXP(GW3)
        I ← I + 1

END
COMMENT  CW ← 0 ;
         FOR I ← 0 STEP 4 UNTIL (1/R) + (R/2) - 6 DO
BEGIN    PRESSURE FORCE ON LINE AB
        CW    ← CW + ((2×R)×(7×FX[I]×CP[I] + 32×FX[I+1]×CP[I+1] +
            12×FX[I+2]×CP[I+2] +32×FX[I+3]×CP[I+3] +
            7×FX[I+4]×CP[I+4]))/45
END
COMMENT  XAB ←0 ;
         FOR I ← 0 STEP 1 UNTIL 1/R + R/2 - 3 DO
BEGIN    COORDINATES ON LINE AB
        XAB ← XAB +((FX[I] + FX[I+1])/2)×R
        WRITE(PRT,FMT2,XAB,CP[I+1])
END
        DTBC ← (K1×CK×P×ST)+2
        DTBC ← ABS(DTBC)
        DTBA1 ← ABS(DTBC)
        PHIB ← -((1/CK)×LN((1/4)×(          DTBA1 + (1/2)×(K1+2))))/2)
        WRITE(PRT,FMT5,PHIB,DTBC,DTBA1)
COMMENT  SUMMATION OF SERIES FOR INTEGRATION ON LINE EDC
        I ← 0
        R ← 0.0125
```

```
REGIN   FOR PHI1 ← 0  STEP R UNTIL  1 + ( R / 2 ) DO
        S10 ← 0 ; S11 ← 0 ; S12 ← 0 ; S13← 0 ; S14← 0 ; S15 ← 0 ;
        S16 ← 0 ; S17 ← 0 ; S18 ← 0 ; S19 ← 0 ; S20 ← 0 ; S21 ← 0 ;
        FOR N ← 1 STEP 1 UNTIL M DO

BEGIN
        S10 ← S10 + ((-1)* N ) × COS( N × PI × PHI1 ) * ( 1 / 2 ) × ( N = Z )
        Q ← Z * ( N )× COS( N × PI × PHI1 ) * ( 1 / 2 ) * ( 1 / 2 )
        S11 ← S11 + ((-1)*(N-1))× SIN( N × PI × PHI1 ) * ( 1 / 2 )
        Q ← Z * ( N )× SIN( N × PI × PHI1 ) * ( 1 / 2 )
        S12 ← S12 + ((-1)*(N-1))× ( 1 / 2 ) = Z
        Q ← * ( N = ( 1 / 2 )
        SIN( N ( 1 / 2 )
        S13 ← S13 + ((-1)*(N-1)) = ( 1/2 )
        Q ← ( N = ( 1 / 2 )
        COS( N ( 1 / 2 )
        S14 ← Q * ( N = Z )
        X × COS( N PI × PHI1 ) * ( N / 2 ) + 2
        COS( N ( 1 / 2 )
        S15 ← S15 + ( N = Z )
        X × SIN( N PI × PHI1 ) * ( N / 2 )
        SIN( N ( 1 / 2 )
        S16 ← S16 + PI × PHI1 )
        COS( N × PI × PHI1 )
        S17 ← Q × PI × ( N = Z )
        SIN( N × PI × PHI1 )
        S18 ← S18 + ((-1)* N )× COS( N × PI × PHI1 ) * ( 2 / PI )* N = Z )× +
        Q ← * ( N )× COS( N × PI × PHI1 ) * ( 2 / PI )
        S19 ← S19 + ((-1)*(N-1))× SIN( N × PI × PHI1 ) * ( 2 / PI )
        Q ← * ( N )× SIN( N × PI × PHI1 ) * ( 2 / PI )
        S20 ← S20 + ((-1)*(N-1))× COS( N × PI × PHI1 ) * ( 2 / PI )× +
        Q ← * ( N )× COS( N × PI × PHI1 ) * ( 2 / PI )
        S21 ← S21 + ((-1)*(N-1))× SIN( N × PI × PHI1 ) * ( 2 / PI )
        Q ← * ( N )× SIN( N × PI × PHI1 ) * ( 2 / PI )

        G3 ← 0 ; H3 ← 0 ;
END     FOR N ← 1 STEP 1 UNTIL 80 DO
```

63

```
BEGIN

G3 + (-4/PI)x((Q+(-N) + Q*N)/((4x(N*2) - 1)x(Q+(-N) - Q*N)))x
SIN(NxPIxPHI1) + G3
H3 + (-4/PI)x(1/(4x(N*2) - 1))xCOS(NxPIxPHI1) + H3

END
COMMENT    PRESSURE DISTRIBUTION ON LINE EDC
VOU +        SQRT((((  1 + S20 )x( 1 + S18 ) + S19 x S21 )
             /((( 1 + S18 )*2 ) + S19 * 2 )          )*2 +
             (( S19 x( 1 + S20 ) - ( 1 + S18 )x S21 ) /((( 1 + S18
             *2 ) + S19 * 2 )                )*2)xEXP(-CxG3)

IF ABS(PIxPHI1 - T) < 0.0001 THEN GO TO L3
A1 + (BxKx(((1+S10)*2)-S11*2))-S12*2+S13*2
A2 + (AxKx(((1+S10)*2)-S11*2))+S12*2-S13*2
B1 + -2xBxKxS11x(1+S10) - 2xS12xS13
B2 + -2xAxKxS11x(1+S10) + 2xS12xS13
C1 + (1+S10)x(1+S16)-S11xS17
C2 + S12xS14 + S13xS15
D1 + -S11x(1+S16)- S17x(1+S10)
D2 + S13xS14 - S12xS15
A3 + (A1xA2 + B1xB2 ) / (A2*2 + B2*2)
B3 + (A2xB1 - A1xB2 ) / (A2*2 + B2*2)
C3 + (C1xC2 + D1xD2 ) / ( C2*2 + D2*2)
D3 + (C2xD1 - C1xD2 ) / ( C2*2 + D2*2)
E3 +((1+S18)x(1+S20) + S19xS21 )/ ((((1+S20)*2) + S21*2)
F3 +(S21x(1+S18) - S19x(1+S20))/ ((((1+S20)*2) + S21*2)
X  +((2xKxCK xA)/(PIxB))x((A3xC3 - B3xD3)xE3 -
(B3xC3 + A3xD3)xF3)
Y  + ( ( 2 x K x CK x A ) / ( PI x B ) ) x
( ( A3 x C3 - B3 x D3 ) x F3 + ( B3 x C3 + A3 x D3 ) x E3 )
FX [ I ] + EXP ( C x G3 ) x( X x COS ( C x H3 ) -
Y x SIN ( C x H3 ) )
FY [ I ] + EXP ( C x G3 ) x( Y x COS ( C x H3 ) +
X x SIN ( C x H3 ) )
GO TO L4
L3: XD + ( = 4x(CK+2)x(1 - BxK2)xAxS19D)/((PI*2)x(A + B)xBx
S21D)
YD + ( 4x(CK+2)x(1 - BxK2)xAx(1 + S18D))/
```

```
        ((PI+2)×B×(A + B)×S21D)
FX [ I ] + EXP ( C × G3 ) ×( XD× COS ( C × H3 ) -
                 YD× SIN ( C × H3 ) )
FY [ I ] + EXP ( C × G3 ) ×( YD× COS ( C × H3 ) +
                 XD× SIN ( C × H3 ) )
L4: I + I + 1
END

        LOD + 0 J CD + 0 J CL + 0 J XEDCOD + 0 J
        SUB + 0 J
        SUBTR + 0
        YEDCOD + 0
COMMENT COORDINATES ON LINE EDC
BEGIN   FOR I + 0   STEP 1 UNTIL   (1/R) + (R/2) - 1 DO

        YEDCOD + YEDCOD + ((R×(FY[I]+FY[I+1]))/2)
        XEDCOD + XEDCOD + ((R×(FX[I]+FX[I+1]))/2)
        WRITE ( PRT , FMT2 , XEDCOD,YEDCOD)
        DY      + YEDCOD - SUBTR
        DX      + XEDCOD - SUB
        LOD + SQRT ( DY + 2 + DX + 2 ) + LOD
        SUB + XEDCOD
        SUBTR + YEDCOD
END

COMMENT FOR I + 0   STEP 8 UNTIL   (1/R) + (R/2) - 8 DO
BEGIN   DETERMINATION OF LIFT AND DRAG COEFFICIENTS BY INTEGRATION

        CD + CD + ((4×R)×(989×FY[I]×CP[I]  + 5888×FY[I+1]×CP[I+1] -
        928×FY[I+2]×CP[I+2] + 10496×FY[I+3]×CP[I+3] - 4540×FY[I+4]×
        CP[I+4] + 10496×FY[I+5]×CP[I+5] - 928×FY[I+6]×CP[I+6] +
        5888×FY[I+7]×CP[I+7] + 989×FY[I+8]×CP[I+8])/14175
        CL + CL + ((4×R)×(989×FX[I]×CP[I] + 5888×FX[I+1]×CP[I+1] -
        928×FX[I+2]×CP[I+2] + 10496×FX[I+3]×CP[I+3] - 4540×FX[I+4]×
        CP[I+4] + 10496×FX[I+5]×CP[I+5] - 928×FX[I+6]×CP[I+6] +
        5888×FX[I+7]×CP[I+7] + 989×FX[I+8]×CP[I+8])/14175
        CD + -CD/LOD J      CL + CL/LOD
        CFP + SQRT ( CD + 2 + CL + 2 )
END
```

```
LDOD ← ( A × ( B - 1 ) ) / ( B × ( 1 + A ) )
DELTAF ← ARCTAN( ( -2 × ( 1 + S7F ) × S8F ) /
( ( ( 1 + S7F ) * 2 ) - S8F * 2 ) ) - C×SSF
IF DELTAF < 0 THEN DELTAF ← DELTAF + PI
CF ← 2 × ( ( 1 - LDOD ) × ( 1 - COS( DELTAF ) ) ) /(LOD))
CC ← LDOD / ( LDOD + YBCOD )
WRITE ( PRT , FMTV )
WRITE ( PRT , FMTKP , LST )

T2 ← (TIME(2) - T2)/60
T3 ← (TIME(3) - T3)/60
WRITE(PRT,FMTIME,T2,T3)

END
END

END
END .
```